THE APPLICATION OF LINEAR OPERATORS TO GEOPHYSICAL PROBLEMS

by

HAROLD POSEN

B.A.Sc., THE UNIVERSITY OF TORONTO

(1952)

SUBMITTED IN PARTIAL FULFILLMENT

OF THE REQUIREMENTS FOR THE

DEGREE OF MASTER OF

SCIENCE

at the

MASSACHUSETTS INSTITUTE OF

TECHNOLOGY

August, 1956

Signature of Author_____
Department of Geology and Geophysics, August 20, 1956

Certified by_____
Thesis Supervisor

Accepted by_____
Chairman, Departmental Committee
on Graduate Students

THE APPLICATION OF LINEAR OPERATORS TO GEOPHYSICAL PROBLEMS

by

Harold Posen

Submitted to the Department of Geology and Geophysics on August 20, 1956 in partial fulfillment of the requirements for the degree of Master of Science.

Fourier transform theory in n dimensions is used to discussthe concept of filtering in observational data which may be a function of more than one variable. The theory is presented for both the continuous and the discrete cases.

As an example of the one-dimensional filter or operator in the discrete case, the problem of resolution of a seismic wavelet complex is examined. The inverse operator, obtained from the inversion of the power series representation of the spectrum of the original wavelet is examined, and its applicability to the resolution of a theoretical seismic complex is studied. A symmetric operator for an actual seismogram is derived and its ability to produce resolution on the seismogram is studied.

The two-dimensional operator is illustrated by deriving an operator suitable for the detection of an anomaly in the presence of noise, in the form of a regional gradient. Two-dimensional spectra and autocorrelation functions are also obtained.

The one-dimensional operators for seismic resolution are found to be only moderately successful, particularly in the noise-free case. However, they do show promise of effective resolving ability in regions other than that studied.

The two-dimensional operator for anomaly detection in the presence of noise is impressively successful in the simple case computed here, and holds great promise for more complex systems of anomalies and noise, if the computational procedure can be mechanized.

The successful application of Fourier transform theory to geophysical data, which may be functions of more than one variable, indicates the possibility for development of

a new interpretative tool. The mathematical development is sufficiently general to hold out a possibility of application of the general concept to any mass of observational data which may be considered a linear combination of noise and signal.

Thesis Supervisor: S. M. Simpson, Jr.
Assistant Professor of Geophysics

TABLE OF CONTENTS

	Page
Abstract	2
Acknowledgements	7
I. Introduction	9
II. Some Aspect of the Theory of the Linear Operator.	12
II.1 Continuous Case	12
II.2 Discrete Case	18
III. The Resolution of a Seismic Wavelet Complex - An Example of a One-Dimensional Operator	22
III.1 Introduction	22
III.2 Specification of the Problem	24
III.3 Resumé of the Theory of the Inverse Operator	25
III.4 The Contractor Operator for the Theoretical Wavelet	27
III.5 The Contractor Operator for a Real Reflection Complex	46
III.6 Conclusions and Recommendations	63
IV. The Removal of Noise in the Interpretation of Potential Field Data - An Example of a Two-Dimensional Operator	65
IV.1 Introduction	65
IV.2 Theory	66
IV.3 The Derivation of the Spiking Operator for the Anomaly due to a Buried Sphere, and Its Application to the Detection of such an Anomaly in the Presence of Noise	72
IV.4 Conclusions and Recommendations	84
V. Concluding Remarks	88
References	90
Figures	
3.1 Ricker wavelets V(25) and V(∞) with their spectral characteristics	31
3.2 Computed inverses to V(25) and V(∞)	32
3.3 Inverses of V(25) and V(∞) showing exponential divergence	33
3.4 Comparisons of re-inverted approximate inverses with original wavelets	34
3.5 Corresponding amplitude and phase spectra	35

TABLE OF CONTENTS

(Continued) Page

Figures

3.6 Comparison of $\frac{1}{V(25)}$ with the inverse of the stable wavelet associated with the amplitude characteristics of V(25)..... 38

3.7 Smoothed inverse operators and their spectral characteristics..... 39

3.8 Convolutions of V(25) and V(∞) with their approximate inverses..... 40

3.9 Artificial wavelet complexes and their resolution by inverse operators..... 41

3.10 Phasing test..... 42

3.11 Results of convolving approximate inverses of V(25) and V(∞) with V(∞) and V(25) respectively..... 45

3.12 Four records of the Atlantic Refining Company exhibiting pinch-out..... 47

3.13 The average wavelet from 7.19 and its spectral characteristics..... 48

3.14 The inverse of the modified wavelet of Figure 3.13..... 49

3.15 The convolution of the 9 term operator with a noise-free wavelet complex from record 7.19... 51

3.16 Convolution of the 9 term operator with various traces of record 7.19..... 52

3.17 The symmetric operator and its amplitude spectrum for the smoothed wavelet..... 55

3.18 The symmetric operator and its amplitude spectrum for the sharp-front wavelet..... 56

3.19 Sharp front wavelet convolved with 49, 25, 15 terms of the symmetric operator of the sharp-front wavelet..... 57

3.20 Smoothed front wavelet convolved with 49, 25, 15 terms of the symmetric operator of the smoothed wavelet..... 58

3.21 Convolution of wavelet of Figure 3.13 with symmetric operator of various lengths..... 59

3.22 Smoothed operator, modified according to the method of Cèsaro sums convolved with sharp-front wavelet..... 60

3.23 A portion of record 7.19 filtered by the symmetric operator formed from the smoothed wavelet..... 61

TABLE OF CONTENTS

(Continued) Page

Figures

3.24 A portion of record 7.19 filtered by the symmetric operator formed from the sharp-front wavelet..... 62

4.1 Anomaly or signal due to buried sphere..... 75
4.2 The combined field of a buried sphere and a south gradient of 40 gravity units per kilometere..... 76
4.3 The operator derived by applying the least squares criterion..... 77
4.4 Autocorrelation function of the signal..... 78
4.5 Wave-number spectrum of the signal..... 79
4.6 Autocorrelation function of the operator..... 80
4.7 Wave-number spectrum of operator..... 81
4.8 Operator convolved with signal..... 82
4.9 Operator convolved with the combined field..... 83
4.10 Section A-A'..... 85
4.11 Section B-B'..... 86

ACKNOWLEDGEMENTS

It gives me great pleasure to express my thanks to Professor S. M. Simpson, Jr. for his aid and encouragement to me during the preparation of this thesis.

I wish to thank the Geophysical Analysis Group under whom the work on seismic resolution was done, and the personnel of that group for their stimulating discussions. Particularly, I appreciate the assistance of Mr. Robert W. Wylie, who worked with me on the problem of seismic resolution (Chapter III), and whose results are incorporated in that chapter.

I am also grateful to Mr. D. R. Grine and Mr. S. Treitel, of the same Group for the use of their Whirlwind I computer programs, which greatly facilitated the numerical work of Chapter III.

I am also grateful to my wife, Annette, for her constant encouragement and careful editing of the final draft of this thesis.

My thanks go also to Mrs. Lillian Christmas for her care and cooperation in the preparation of the final copies of this thesis.

This thesis was prepared while I held an Ontario Research Council Scholarship. I am indeed grateful to

the Ontario Research Council for making this year of graduate study and research possible.

I. INTRODUCTION

In the course of a scientific investigation, be it an experiment in the laboratory, or a geophysical survey in some remote area, vast amounts of data are obtained, and the investigator is often faced with the problem of separating the wheat from the chaff, or, in the language of the electrical engineer, the signal from the noise.

Unfortunately, the term noise, possibly because of its popular description as a disturbance, random in nature, would appear to be ambiguous in the light of the following analysis; consequently, a definition would not be out of place at this time. We will define noise as that part of the observational data which represents undesirable signal content. It is not necessarily random in nature. It should be pointed out that what may represent undesired signal in one instance may be the desired signal in another. A good example of this is found in a gravity survey interpretation, where regional and terraine effects (usually non-random in nature) are considered undesirable signal (noise) and consequently something to be removed from the data. Depending upon the desired information, the effects of the basement configuration or shallower horizons may be considered undesirable signal.

Now the interpreter, once he has made his decision as to what constitutes the noise and what the signal, for his

particular purpose, has yet to design a device to remove the noise, and to interpret the noise-free signal. This thesis will be primarily concerned with some aspects of the problem of noise removal in data which can be considered a linear combination of signal and noise.

Perhaps the most fruitful approach to the noise elimination problem has been in the methods of the communication engineer with their emphasis on filtering techniques.

This approach, embodying much of the theory of generalized harmonic analysis (Wiener, 1950) has been promulgated by the Geophysical Analysis Group at the Massachusetts Institute of Technology. The emphasis here has been on the derivation of suitable mathematical linear operators (which can be shown to be the analogue in the discrete case of the electrical filter in the continuous case - Smith, 1952), which operate on data in such a way that the undesirable signal is removed, or minimized in the sense of a satisfactory criterion. Most of the work has been confined to exploration seismology, essentially a one-dimensional phenomenon in that the data is usually considered a function of time only. The possibility of extending this communication engineering approach to more than one dimension has been investigated by Smith (1952), who developed a two-dimensional linear operator for a set of seismic traces. Schwartz (1954) also uses this communication engineering approach in his paper on residual

maps, but makes no mention of the application of linear operators.

The purpose of this thesis is to indicate the possibility of extending the methodology to data which may be a function of more than one variable, and to give the results of two groups of experiments, illustrating the derivation and application of one-dimensional and two-dimensional linear operators as noise filters (in the sense defined above). The term experiments is used advisedly, because, although the mathematical formulation of the operator is quite exact, the derivation of a suitable operator (e.g. an operator containing less than an infinite number of terms) is often the result of trial and error and informed intuition. This will be particularly evident in our examination of a suitable one-dimensional operator for contracting a seismic wavelet.

II. SOME ASPECTS OF THE THEORY OF THE LINEAR OPERATOR

II.1. Continuous Case

Geophysical data, or, for that matter, any observational data, can be represented by a function $m(\underline{x})$, where $\underline{x}$ is an n-dimensional vector. The dimensions of $\underline{x}$ depend on the variety of observations made. In seismology $\underline{x}$ is usually considered a one-dimensional variable, time. In potential field investigations, $m(\underline{x})$ may be considered a function of two variables. Here $m(\underline{x})$ would represent the value of the potential field at a pt $\underline{x} = (x_1, x_2)$ on the earth's surface. In other instances $m(\underline{x})$ may be a function of more than two variables, as in a core-hole survey in which temperature or mineralization is measured as a function of the three space coordinates, and lithology.

The Fourier transform of a function of one variable is a function of the reciprocal of that variable, and is termed a spectrum. For example, a function of time, becomes, under transformation, a function of reciprocal time or frequency. Analogously, the Fourier transform of a function of n variables gives us a function in terms of the reciprocals of those variables. Since, in most geophysical observations, the data $m(\underline{x})$ is a function of the space coordinates, we will call the transform of the data, $M(\underline{k})$, a wave-number (reciprocal-length) spectrum. $\underline{x}$ and $\underline{k}$ are n-dimensional vectors with components $(x_1, x_2, \ldots\ldots, x_n)$ and $(k_1, k_2, \ldots\ldots, k_n)$ respectively.

Let it be assumed that $m(\underline{x})$ is a well-behaved function (its n derivatives exist and are continuous). This assumption can be considered valid for practically all physical data. Let it also be assumed that $m(\underline{x})$ is "integrable square" over the n-dimensional space, and hence it can be represented by its Fourier transform, and that outside the region in which $m(\underline{x})$ is defined, it is everywhere zero.

Then

$$m(\underline{x}) = \int_{-\infty}^{\infty} M(\underline{k}) e^{i(\underline{k}\cdot\underline{x})} d\underline{k} \qquad (2.1.1)$$

$$M(\underline{k}) = \frac{1}{(2\pi)^n} \int_{-\infty}^{\infty} m(\underline{x}) e^{-i(\underline{k}\cdot\underline{x})} d\underline{x}. \qquad (2.1.2)$$

The integration is over n-dimensional space, and

$$d\underline{x} = dx_1 dx_2 \ldots\ldots dx_n$$

$$d\underline{k} = dk_1 dk_2 \ldots\ldots dk_n$$

$$\underline{k}\cdot\underline{x} = k_1x_1 + k_2x_2 + \ldots\ldots + k_nx_n, \text{ the dot product.}$$

Now, a linear constant element filter, or some operation on the data, may be characterized by its impulse response function $h(\underline{y})$, where $\underline{y}$ is the n-dimensional vector with components $(y_1, y_2, \ldots, y_n)$.

Suppose the observed data $m(\underline{x})$ is operated upon by such a filter. The result of this operation is given by the convolution integral, for the process of convolution may also be extended to n-dimensional space (Titmarsh, 1948), and hence $g(\underline{x})$, the output or filtered data, is given by

$$g(\underline{x}) = h(\underline{y}) * m(\underline{x}) = \int_{-\infty}^{\infty} m(\underline{x}-\underline{y})h(\underline{y})d\underline{y} \qquad (2.1.3)$$

where, as before, integration is over n-dimensional space, and $d\underline{y} = dy_1 dy_2 \ldots dy_n$.

The wave-number spectrum of the output, $G(\underline{k})$, is given by

$$G(\underline{k}) = \frac{1}{(2\pi)^n} \int_{-\infty}^{\infty} g(\underline{x})e^{-i(\underline{k}\cdot\underline{x})}d\underline{x} \qquad (2.1.4)$$

$$= \frac{1}{(2\pi)^n} \int_{-\infty}^{\infty} h(\underline{y})d\underline{y} \int_{-\infty}^{\infty} m(\underline{x}-\underline{y})e^{-i(\underline{k}\cdot\underline{x})}d\underline{x}. \qquad (2.1.5)$$

In the integral in which $\underline{y}$ is considered constant, let $\underline{z} = \underline{x}-\underline{y}$.

Then $$G(\underline{k}) = \frac{1}{(2\pi)^n} \int_{-\infty}^{\infty} h(\underline{y})e^{-i(\underline{k}\cdot\underline{y})}d\underline{y} \int_{-\infty}^{\infty} m(\underline{z})e^{-i(\underline{k}\cdot\underline{z})}d\underline{z}$$

$$= H(\underline{k})M(\underline{k}) \qquad (2.1.6)$$

where $H(\underline{k})$ is the wave-number spectrum of the impulse response function $h(\underline{y})$, or

$$H(\underline{k}) = \frac{1}{(2\pi)^n} \int_{-\infty}^{\infty} h(\underline{y})e^{-i(\underline{k}\cdot\underline{y})}d\underline{y}. \qquad (2.1.7)$$

Hence, if the spectral characteristics of the data and the filter are known, the spectrum of the filtered output may be obtained by a multiplication, rather than by an integration. The advantage of working in the $\underline{k}$ domaine becomes more apparent if several filtering operations are used. As an example, let us consider gravity observations. The observed

data $m(\underline{x})$ is usually treated for the Bouger effect, terraine, and regional effects. When these effects are linear, then the net result of these operations on our data may be considered the result of successive filtering operations on $m(\underline{x})$.

Suppose the impulse responses of these various operations are $h_B(\underline{y})$, $h_t(\underline{y})$ and $h_r(\underline{y})$ respectively, then the wave-number spectrum of the result of these operations is $H_B(\underline{k})H_t(\underline{k})H_r(\underline{k})M(\underline{k})$, or, in the $\underline{x}$ domaine,

$$h_B*h_t*h_r*m = \int_{-\infty}^{\infty} h_B(\underline{a}) \int_{-\infty}^{\infty} h_t(\underline{b}) \int_{-\infty}^{\infty} h_r(\underline{c})m(\underline{x}-\underline{c}-\underline{b}-\underline{a})d\underline{a}d\underline{b}d\underline{c}$$

$$= \int_{-\infty}^{\infty} e^{-i(\underline{k}\cdot\underline{x})} H_B(\underline{k})H_t(\underline{k})H_r(\underline{k})M(\underline{k})d\underline{k}. \qquad (2.1.8)$$

The cross-correlation function $\varphi_{12}(\underline{y})$ of two functions $m_1(\underline{x})$ and $m_2(\underline{x})$ is defined by

$$\varphi_{12}(\underline{y}) = \lim_{T\to\infty} \frac{1}{(2T)^n} \int_{-T}^{T} m_1(\underline{x})m_2(\underline{x}+\underline{y})d\underline{x} \qquad (2.1.9a)$$

or, for functions which are transient in behavior,

$$\varphi_{12}(\underline{y}) = \int_{-\infty}^{\infty} m_1(\underline{x})m_2(\underline{x}+\underline{y})d\underline{x}. \qquad (2.1.9b)$$

For observational data which represent local phenomena, and have a finite total energy, equation (2.1.9b) is the proper representation of the cross-correlation function. Equation (2.1.9a) would be used for phenomena which persist over all space.

Now $$\varphi_{12}(\underline{y}) = \int_{-\infty}^{\infty} m_1(\underline{x}) m_2(\underline{x}+\underline{y}) d\underline{x}$$

$$= \int_{-\infty}^{\infty} m_1(\underline{x}) d\underline{x} \int_{-\infty}^{\infty} M_2(\underline{k}) e^{i\underline{k}\cdot(\underline{x}+\underline{y})} d\underline{k}$$

$$= \int_{-\infty}^{\infty} M_2(\underline{k}) e^{i(\underline{k}\cdot\underline{y})} d\underline{k} \int_{-\infty}^{\infty} m_1(\underline{x}) e^{i(\underline{k}\cdot\underline{x})} d\underline{x}. \qquad (2.1.10)$$

But

$$\int_{-\infty}^{\infty} m_1(\underline{x}) e^{i(\underline{k}\cdot\underline{x})} d\underline{x} = (2\pi)^n \overline{M_1(\underline{k})} \qquad (2.1.11)$$

where the bar indicates complex conjugate.

$$\therefore \varphi_{12}(\underline{y}) = \int_{-\infty}^{\infty} \left[(2\pi)^n \overline{M_1(\underline{k})} M_2(\underline{k})\right] e^{i(\underline{k}\cdot\underline{y})} d\underline{k}. \qquad (2.1.12)$$

Following Lee's (1956) definition for functions of one-dimensional variables, let

$$\Phi_{12}(\underline{k}) = (2\pi)^n \overline{M_1(\underline{k})} M_2(\underline{k}) \qquad (2.1.13)$$

be the cross wave-number spectrum of $m_1(\underline{x})$ and $m_2(\underline{x})$ for functions of n-dimensional variables.

Then

$$\varphi_{12}(\underline{y}) = \int_{-\infty}^{\infty} \Phi_{12}(\underline{k}) e^{i(\underline{k}\cdot\underline{y})} d\underline{k} \qquad (2.1.14)$$

and

$$\Phi_{12}(\underline{k}) = \frac{1}{(2\pi)^n} \int_{-\infty}^{\infty} \varphi_{12}(\underline{y}) e^{-i(\underline{k}\cdot\underline{y})} d\underline{y}. \qquad (2.1.15)$$

Now, if $m_1(\underline{x}) = m_2(\underline{x}) = m(\underline{x})$, then

$$\varphi_{12}(\underline{y}) = \varphi_{11}(\underline{y}) = \int_{-\infty}^{\infty} m(\underline{x})m(\underline{x}+\underline{y})d\underline{x}. \qquad (2.1.16)$$

$\varphi_{11}(\underline{y})$ is termed the autocorrelation function of $m_1(\underline{x})$ and

$$\Phi_{12}(\underline{k}) = \Phi_{11}(\underline{k}) = (2\pi)^n \overline{M_1(\underline{k})} M_1(\underline{k}) = (2\pi)^n \left|M_1(\underline{k})\right|^2. \qquad (2.1.17)$$

Then

$$\varphi_{11}(\underline{y}) = \int_{-\infty}^{\infty} \Phi_{11}(\underline{k}) e^{i(\underline{k}\cdot\underline{y})} d\underline{k} \qquad (2.1.18)$$

and

$$\Phi_{11}(\underline{k}) = \frac{1}{(2\pi)^n} \int_{-\infty}^{\infty} \varphi_{11}(\underline{y}) e^{-i(\underline{k}\cdot\underline{y})} d\underline{y}. \qquad (2.1.19)$$

Now, for $\underline{y} = 0$

$$\varphi_{11}(0) = \int_{-\infty}^{\infty} m^2(\underline{x})d\underline{x} = \int_{-\infty}^{\infty} \Phi_{11}(\underline{k})d\underline{k} \qquad (2.1.20)$$

which is Parseval's relation.

$\int_{-\infty}^{\infty} m^2(\underline{x})$ may be considered the total energy of the data $m(\underline{x})$, and hence $\Phi_{11}(\underline{k}) = (2\pi)^n \left|M(\underline{k})\right|^2$ can be considered the energy density spectrum in its broadest sense.

Since the autocorrelation function is an even function,

$$\varphi_{11}(\underline{y}) = \int_{0}^{\infty} \Phi_{11}(\underline{k}) \cos(\underline{k}\cdot\underline{y})d\underline{k} \qquad (2.1.21)$$

$$\Phi_{11}(\underline{k}) = \frac{1}{(2\pi)^n} \int_{0}^{\infty} \varphi_{11}(\underline{y}) \cos(\underline{k}\cdot\underline{y})d\underline{y}. \qquad (2.1.22)$$

In reality, the data $m(\underline{x})$ can seldom be expressed as a continuous function, but is usually expressed as a function of some discrete variable.

II.2. Discrete Case

The discrete theory for the one-dimensional case has been well-documented, and although Smith (1952) develops many of the relations for the two-dimensional operators, it is felt that, for the sake of completeness, a brief survey of the n-dimensional operators should be included. It is doubtful whether operators of greater than three dimensions will ever be used, primarily because of computational difficulties, but this non-rigorous development of the n-dimensional operator is included for academic completeness.

Smith shows that the convolution integral in one dimension (equation (2.1.3) with n = 1) can be approximated by a series

$$g(\underline{x}) \simeq g(ih) = \sum_{s_1=-a_1}^{b_1} a_{s_1} m_{i_1-s_1} \qquad (2.2.1)$$

where a_{s_1} represents h times the impulse response of our filter and the totality of terms a_{s_1} is called the linear operator. He also suggests extending this form to operators of dimensions greater than one, and for the purpose of this development, we accept this suggestion as both a reasonable and valid extrapolation of (2.2.1).

Then the result of operating on our data m_{i_1} with a filter (or operator) whose general term is $a_{\underline{s}}$ is

$$g_{\underline{ih}} = \sum_{s_1 = a_1}^{b_1} \cdots\cdots \sum_{s_n = a_n}^{b_n} a_{\underline{s}} m_{\underline{ih}-\underline{s}} \qquad (2.2.2)$$

where $\underline{ih} = (i_1h_1, i_2h_2, \ldots i_nh_n)$, $\underline{s} = (s_1, s_2, \ldots s_n)$, and $\underline{ih}-\underline{s} = (i_1h_1-s_1, i_2h_2-s_2 \ldots i_nh_n-s_n)$ and where $g_{\underline{ih}}$ is the output of the filter at the point $\underline{x} = \underline{ih} = (i_1h_1, i_2h_2, \ldots, i_nh_n)$. $h_1, \ldots h_n$ are the spacings between the successive data points in each of the n dimensions, and i_k is a running integer.

Let the wave-number spectrum of the discrete data $m(\underline{ih})$ be $M(\underline{k}) = M(\underline{jt})$ where $\underline{k} = \underline{jt} = (j_1t_1, j_2t_2 \ldots j_nt_n)$ $t_1, \ldots t_n$ are the spacing constants in $\underline{k}$ domaine, and j_k is a running integer.

$$M_{\underline{jt}} = \sum_{i_1} \cdots\cdots \sum_{i_n} m_{\underline{ih}} e^{-i(\underline{jt}\cdot\underline{ih})}. \qquad (2.2.3)$$

In the $\underline{x}$ domaine

$$m_{\underline{ih}} = \sum_{j_1} \cdots\cdots \sum_{j_n} M_{\underline{jt}} e^{i(\underline{jt}\cdot\underline{ih})}. \qquad (2.2.4)$$

Now the wave-number spectrum of the filtered output is $G(\underline{k})$.

$$G(\underline{k}) = G(\underline{jt}) = \sum_{i_1} \cdots\cdots \sum_{i_n} g_{\underline{ik}} e^{-i(\underline{jt}\cdot\underline{ih})} \qquad (2.2.5)$$

$$= \sum_{i_1} \cdots\cdots \sum_{i_n} \left(\sum_{s_1} \cdots\cdots \sum_{s_n} a_{\underline{s}} m_{\underline{ih}-\underline{s}} \right) e^{-i(\underline{jt}\cdot\underline{ih})}.$$

Let $\underline{ih}-\underline{s} = \underline{z}$, then

$$G(\underline{k}) = \sum_{s_1} \cdots \sum_{s_n} a_{\underline{s}} e^{-i(\underline{jt}\cdot\underline{s})} \left(\sum_{z_1 + s_1} \cdots \sum_{z_n + s_n} m_{\underline{z}} e^{-i(\underline{jt}\cdot\underline{z})} \right)$$

$$G(\underline{k}) = A(\underline{k})M(\underline{k}) \qquad (2.2.6)$$

where $A(\underline{k}) = A(\underline{jt})$ is the wave-number spectrum of our operator.

$$A(\underline{k}) = \sum_{s_1} \cdots \sum_{s_n} a_{\underline{s}} e^{-i(\underline{k}\cdot\underline{s})}. \qquad (2.2.7)$$

Hence, the relationship among the spectral characteristics of the data, operator, and output holds in the discrete case as well as in the continuous case.

The autocorrelation function in the discrete case is defined as

$$\varphi_{11}(\underline{s}) = \sum_{i_1 = 0}^{a_1 - s_1} \cdots \sum_{i_n}^{a_n - s_n} m_{\underline{ih}} m_{\underline{ih} + \underline{s}}. \qquad (2.2.8)$$

Now, the spectrum of $m_{\underline{ih} + \underline{s}} = \sum_{i_1} \cdots \sum_{i_n} m_{\underline{ih} + \underline{s}} e^{-i(\underline{k}\cdot\underline{ih})}$ where $\underline{s}$ does not enter into the summation.

Let $\underline{ih} + \underline{s} = \underline{z}$; then the spectrum of $m_{\underline{ih} + \underline{s}}$ is

$$\sum_{z_1 - s_1} \cdots \sum_{z_n - s_n} m_{\underline{z}} e^{-i(\underline{k}\cdot\underline{z} - \underline{k}\cdot\underline{s})}$$

$$= e^{+i\underline{k}\cdot\underline{s}} \sum_{z_1-s_1} \cdots \sum_{z_n-s_n} m_{\underline{z}} e^{-i(\underline{k}\cdot\underline{z})} = e^{i\underline{k}\cdot\underline{s}} M(\underline{k}) \qquad (2.2.9)$$

where $M(\underline{k})$ is the wave-number spectrum of $m_{\underline{ih}}$.

$$\therefore \varphi_{11}(\underline{s}) = \sum_{i_1} \cdots \sum_{i_n} m_{\underline{ih}} \left(\sum_{k_1} \cdots \sum_{k_n} M_{\underline{k}} e^{i\underline{k}\cdot(\underline{ih}+\underline{s})} \right) =$$

$$\sum_{k_1} \cdots \sum_{k_n} M_{\underline{k}} e^{i\underline{k}\cdot\underline{s}} \left(\sum_{i_1} \cdots \sum_{i_n} m_{\underline{i}} e^{i\underline{k}\cdot(\underline{ih})} \right)$$

but $\sum_{i_1} \cdots \sum_{i_n} m_{\underline{i}} e^{i\underline{k}\cdot(\underline{ih})} = \overline{M(\underline{k})}$.

$$\therefore \varphi_{11}(\underline{s}) = \sum_{k_1} \cdots \sum_{k_n} \overline{M(\underline{k})} M(\underline{k}) e^{i\underline{k}\cdot\underline{s}}. \qquad (2.2.10)$$

If we let $\Phi_{11}(\underline{k}) = \overline{M(\underline{k})} M(\underline{k}) = |M(\underline{k})|^2$ be the energy density spectrum as before, then

$$\varphi_{11}(\underline{s}) = \sum_{k_1} \cdots \sum_{k_n} \Phi_{11}(\underline{k}) e^{i\underline{k}\cdot\underline{s}} \qquad (2.2.11)$$

and

$$\Phi_{11}(\underline{k}) = \sum_{s_1} \cdots \sum_{s_n} \varphi_{11}(\underline{s}) e^{-i\underline{k}\cdot\underline{s}}. \qquad (2.2.12)$$

Apparently, analogous relations can be obtained for the discrete case to those for the continuous case.

III. THE RESOLUTION OF A SEISMIC WAVELET COMPLEX - AN EXAMPLE OF A ONE-DIMENSIONAL OPERATOR

III.1. Introduction

Better resolution has always been the desire of the practicing seismologist, but until recently instrumentation and interpretative techniques, in general proved quite adequate. However, in recent years with the expansion of oil exploration into areas such as the Williston Basin, where oil accumulations appear to be controlled, in the main, by stratigraphy rather than structure, the need for techniques whereby overlapping seismic reflections could be resolved, became of paramount importance.

The approach by the industry to this problem has been essentially mechanical in nature with the emphasis on instrumentation (the so-called "high-resolution" instruments) and visual aids in the form of reduced record sections, not on new interpretative techniques.

Actually the problem of resolution is a problem of noise minimization, for the difficulty lies not in picking the earliest reflection of a wavelet complex, but in distinguishing the arrival times of the later events, which may be masked by the energy of the first. Hence, a desirable "modus operandi" for improving resolution would be to suppress the initial reflection of the complex, which in this instance is regarded as the undesirable signal (noise), or, barring that, to reduce the time expression of the undesirable wave,

in order that the following reflection may be distinguished.

The process of reducing the time expression of the reflection, or contraction as we shall call it, appears to offer the best solution to the problem, for ideally it would permit the separation of the members of the complex, and still retain their relation to one another in the time domaine. In practice, contraction offers the only solution to the problem, since in most cases the members of a wavelet complex differ by so little in their frequency content that suppression by electrical filters is virtually impossible. As a result, the work done on improving resolution has centred upon designing suitable mathematical contractor methods.

Ricker (1953b) proposed and built an electrical filter, based on his wavelet theory of seismogram structure (Ricker, 1953a), with which he achieved some resolution of the component wavelets of a complex by contracting the individual wavelets to 0.8 of their original breadth, and still retained their individual wavelet shapes. Unfortunately, the wavelet theory has fallen into disrepute of late, and the applicability of his contractor to other than highly specialized cases is in doubt.

In view of these developments, it was felt that the possibility of obtaining new, and perhaps better means of resolution should be investigated.

III.2. Specification of the Problem

Ideally, we would like to find some mathematical filter or operator whereby a reflection complex consisting of the superposition of two or more reflections can be resolved into its component reflections with a minimum distortion of the interpretational characteristics. Interpretational characteristics may be considered as those features of a seismic reflection, by which it may be identified and mapped. These characteristics are wave-shape, phasing and the various other undefinables that constitute reflection "character," and the inception or arrival time of the reflection. Undoubtedly, the most important of these is the arrival time, for without it, the reflection could not be accurately mapped.

Although the variation in wave-shape of a reflection throughout an area must contain important information as to lithology (at present this information is not interpretable, except in vague generalities), it is not a prerequisite in mapping the reflection, particularly in these days of continuous profiling. Consequently, we may relax the specification of minimum alteration of wave-shape for our mathematical filter, and restate our problem as: the determination of an operator (filter), by which a reflection complex can be separated into its components by contraction with a minimum distortion of the individual arrival times.

III.3. Resume of the Theory of the Inverse Operator

Relaxation of the restriction as to retention of wave-shape after filtering, permits a wider choice in the form of our filtered output. Perhaps the best mathematical representation of our filtered output would be a spike or impulse function, which, because of its zero width, could exactly represent the arrival time of the reflection in the time-domaine (in this section $\underline{x}$ represents the one-dimensional variable time) and the ultimate in contraction. Now a spike in the time-domaine is represented by a constant in the frequency domaine ($\underline{k}$ domaine), or as it is often called a white-light spectrum (Guilleman, 1949). This representation in the frequency domaine has some fortunate mathematical advantages, for as we have shown, the spectrum of the filtered output $G(\underline{k})$ is the product of the individual spectra of the operator and data.

$$G(\underline{k}) = A(\underline{k})M(\underline{k})$$

Hence, to obtain a white-light spectrum and thereby a spike in the time-domaine, the operator spectrum $A(\underline{k})$ should equal $1/M(\underline{k})$, and therefore the output $G(\underline{k}) = A(\underline{k})M(\underline{k}) = \frac{1}{M(\underline{k})}.M(\underline{k}) = 1$, a constant.

Robinson (1953) demonstrates that the spectrum of the operator $A(\underline{k}) = \sum_{s=0}^{m} a_s e^{-ik\underline{s}}$ may be represented by a power series in z

$$A(\underline{z}) = \sum_{s=0}^{m} a_s e^{-iks} = \sum_{s=0}^{m} a_s z^s = \tag{3.3.1}$$

$$a_0 + a_1 z + a_2 z^2 + \ldots + a_m z^m.$$

He also shows that this operator will be stable (the roots of the associated difference equation damp to zero) if the roots z_k of this polynomial fall outside the unit circle in the z plane, or that A(z) is analytic for $|z| \leq 1$, and consequently the inverse operator $A^{-1}(z) = 1/A(z) = \dfrac{1}{\sum_s a_s z^s} = B(z)$ exists and is analytic for $|z| \leq 1$, and hence may also be expanded as a power series in z, or

$$A^{-1}(z) = \frac{1}{\sum_{s=0}^{m} a_s z^s} = \sum_{t=0}^{\infty} b_t z^t = B(z). \tag{3.3.2}$$

The coefficients of the inverse operator may be found by direct division of the polynomial $\sum_{s=0}^{m} a_s z^s$ into unity.

The basis of our experimental technique was to obtain a representative wavelet of the initial reflection of the complex, and then considering this wavelet as the operator, characterizing the undesirable signal or noise, obtain its inverse and use this to operate in our complex, in the hope that the result of this operation (obtained by convolving the operator with the complex, according to equation (2.2.2)) will contract the initial wavelet to a spike at its inception time with a minimum of energy before and after the spike, thus

permitting the accurate determination of the arrival times of the later reflections in the complex.

The general plan of the experiments was to derive a suitable inverse for a wavelet, representative of a theoretical reflection. (In this instance, the wavelet chosen was the Ricker wavelet, (III.4)). Then after testing its effectiveness on a theoretical complex, it was intended to extend the results to a reflection complex obtained from an actual seismogram (III.5). Here we find that slightly different techniques are required to obtain suitable operators.

III.4. The Contractor Operator for the Theoretical Wavelet

The inverse operator, whose spectrum is B(z) contains an infinite number of operator coefficients (equation (3.3.2)), and hence would be impracticable as a contractor, unless the coefficients of the higher powers of z became negligibly small and can be neglected. Unfortunately, the representation as a power series in z of the spectral characteristics of the inverse wavelets found in practice gives rise to a diverging sequence of operator coefficients. However, the inverse formulation of the operator represents the most desirable contractor operator (see above), and as such the inverse form should be retained, perhaps by approximating the inverse by the first few terms of the sequence before they become widely divergent (Dr. Piety, 1955). The convolution of such "chopped-off" inverses and the original operator should produce a spike, valid at least to the number of terms retained

in the inverse.

Ricker's presentation of his wavelet theory of seismogram structure and tables of typical wavelets (1953a) offered an opportunity to test the hypothesis of practical "chopped-off" inverses and enabled us to compare some of the properties of his theoretical wavelets with those of the wavelets found on a seismogram.

Ricker wavelets V(25) and V(∞) were chosen as operators, where V(25) represents the Ricker wavelet at 25 dimensionless units from the source and V(∞), the Ricker wavelet at an infinite distance from the source. These wavelets extend in time from minus infinity to plus infinity with V(∞) symmetrical in shape and V(25) non-symmetrical in shape. In order to have wavelets more representative of physical reality, the Ricker wavelets were modified so as to start at a time origin with a discrete jump in amplitude. It was felt that the jump at the origin would be representative of the initial impulse, which characterizes the true reflection (Fig. 3.1).

Figure 3.2 shows the computed inverses of V(25) and V(∞), designated as $\frac{1}{V(25)}$ and $\frac{1}{V(\infty)}$ respectively to 180 terms. Both inverses exhibit the expected divergence, and in both instances the major share of this divergence was recognized to be due to an exponential function superimposed on some function characteristic of the individual inverse. The semi-log plot of Figure 3.3 illustrates this exponential divergence

and permits the calculation of these functions ae^{bx}, where a and b are constants, characteristic of the individual wavelets. Since, according to our hypothesis, only the first few terms of our inverse are to be used as the contractor operator, the exponential functions were removed by subtraction from their respective inverses, in the hope that the resultant inverses $\frac{1}{V(s)} - ae^{bx}$. (We shall use V(s) as a generic term for either V(25) or $V(\infty)$, when possible), would contain a larger number of useable terms.

It was realized, however, that the positive intercept, a, of the exponential function ae^{bx} represented the inverse of the first term of the original operator or wavelet, and as such it should not be removed from the inverse, in order to retain the discrete jump at the origin of the wavelet. Our inverse operator, modified according to these precepts, then becomes

$$\frac{1}{V(s)} - a(e^{bx}-1).$$

This operator will be referred to as the modified inverse operator, or modified inverse.

Figure 3.4 is a comparison of the re-inverted operators. $\frac{1}{\frac{1}{V(s)} - ae^{bx}}$, $\frac{1}{\frac{1}{V(s)} - a(e^{bx}-1)}$ with the original operators and shows the importance of retaining the intercept term "a" in the modified inverse. The re-inverted inverse $\frac{1}{\frac{1}{V(s)} - ae^{bx}}$

bears little, if any relation to the original wavelet V(s), while the re-inverted inverse $\frac{1}{\frac{1}{V(s)} - a(e^{bx}-1)}$ approximates the original wavelet, fairly closely, aside from end effects.

A symmetric wavelet (operator and wavelet are used interchangeably throughout this discussion), like V(∞) has an inverse which is non-stable (the representation of the wavelet in discrete form is not a solution of a stable difference equation), and hence the stability of a symmetric wavelet is non-stable (M.I.T. G.A.G. Report No. 9). The wavelet V(25), although asymmetric is also non-stable, as can be seen from its divergent inverse (Fig. 3.2). However, Robinson (1953) shows that the power spectrum $\Phi(\omega) = |B(\omega)|^2 = B(\omega)\overline{B(\omega)}$ of an unstable operator may be factored by the Wold-Kolmogoroff method to yield a spectrum, whose representation in the time domaine gives a stable operator. Thus, an unstable wavelet whose spectrum is $B^2(\omega)$ has associated with it a stable wavelet whose spectrum is also $B^2(\omega)$.

In view of this, and the experimental evidence that the two inverses examined consist of some function, characteristic of the individual wavelet, superimposed on a divergent exponential function, it was felt that the function characterizing the wavelet may be associated with the stable wavelet, derivable from the original wavelet by spectral factorization (Fig. 3.5).

A comparison of the inverse wavelet $\frac{1}{V(25)}$, and the inverse of the associated stable wavelet of V(25) appears to

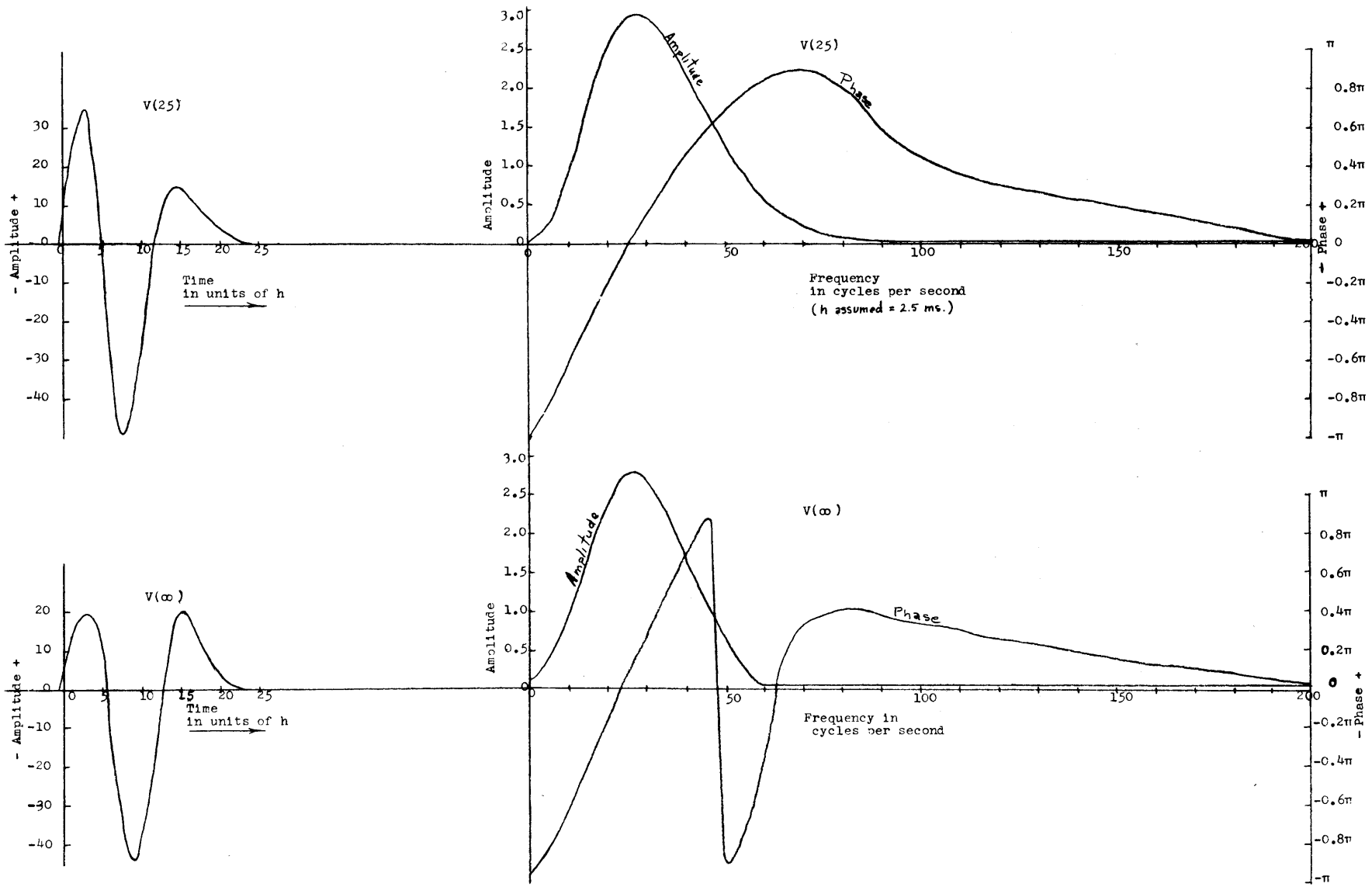

Fig. 3.1 Ricker Wavelets V(25) and V(∞) with their spectral characteristics.

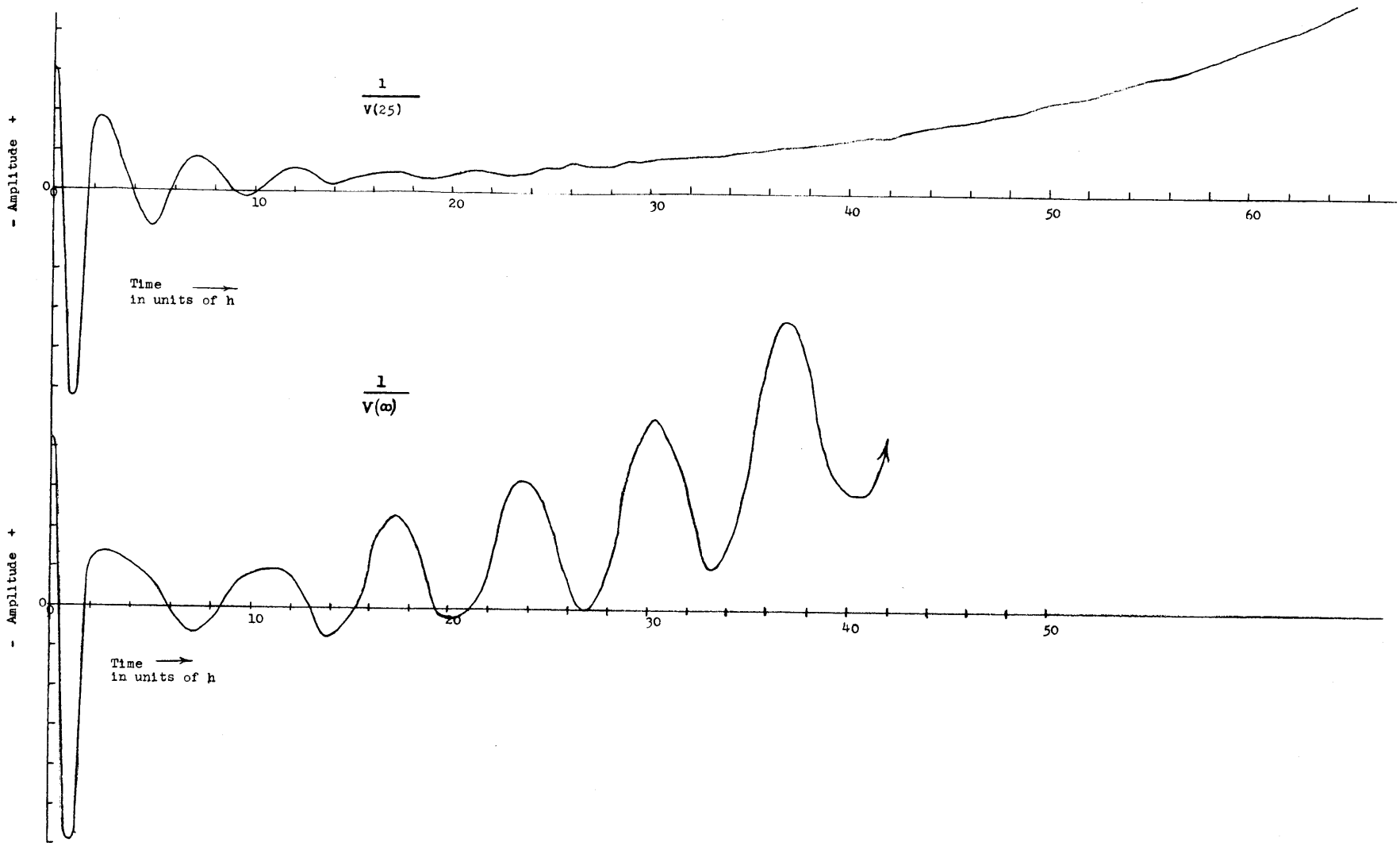

Fig. 8.2. Computed inverses to V(25) and V(∞) of Fig. 8.1.

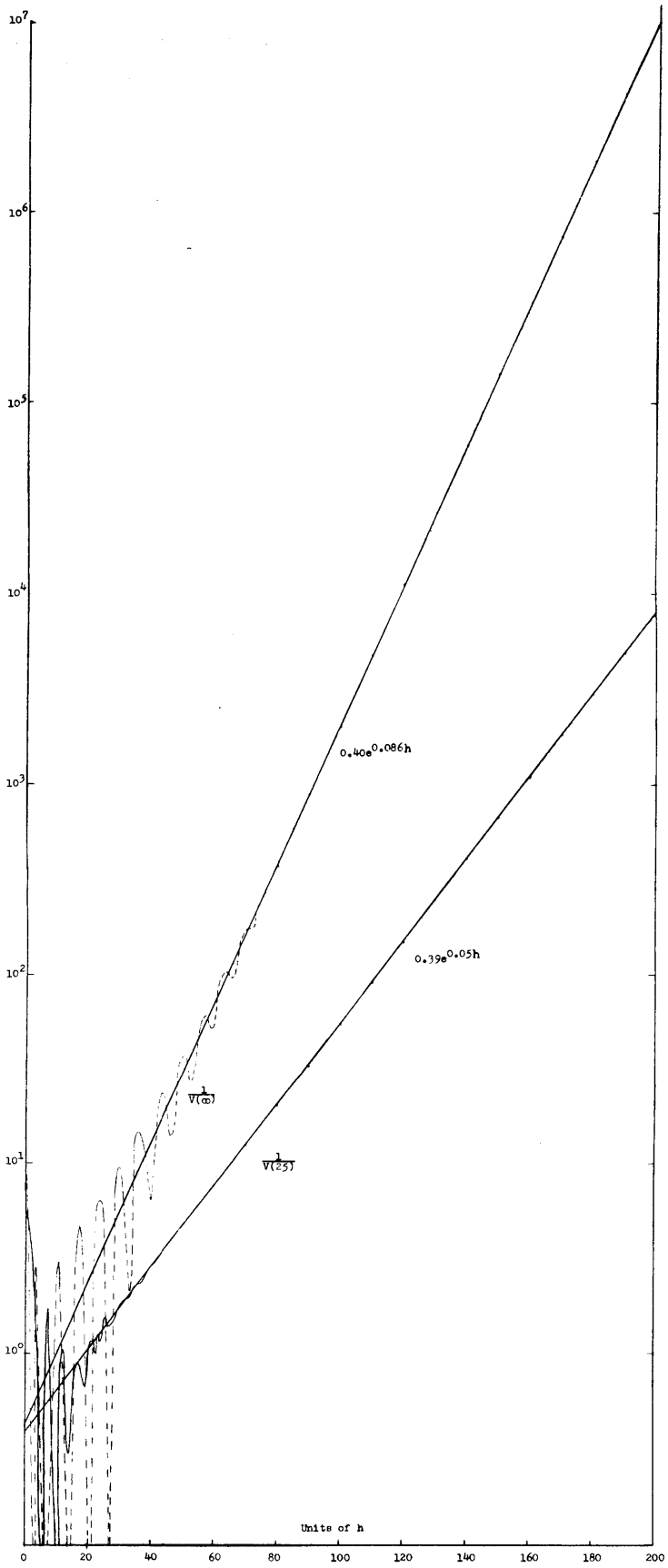

Fig. 3.3 Inverses of V(25) and V(∞) showing exponential divergence

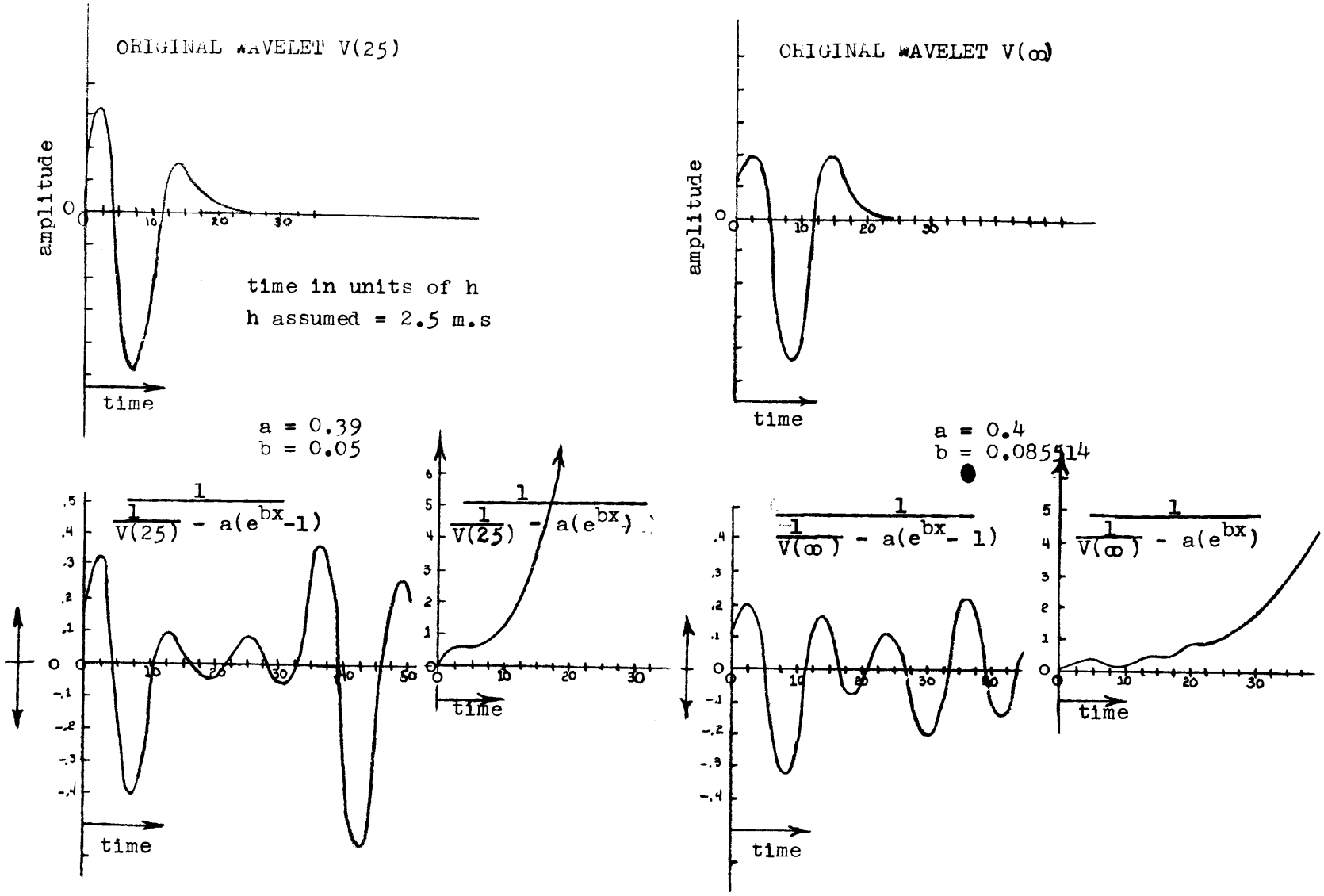

Fig. 3.4 Comparisons of re-inverted approximate inverses with original wavelets

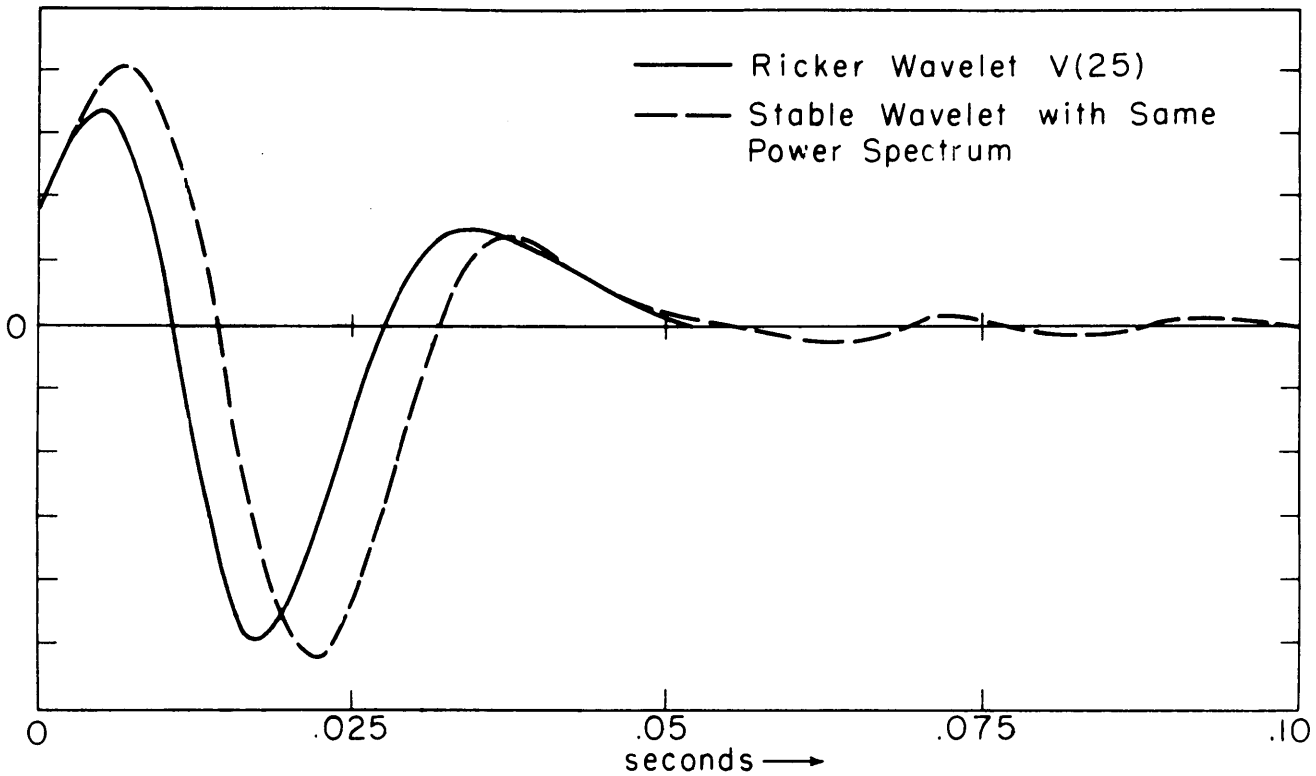

FIG. 3.5 STABLE AND UNSTABLE WAVELETS

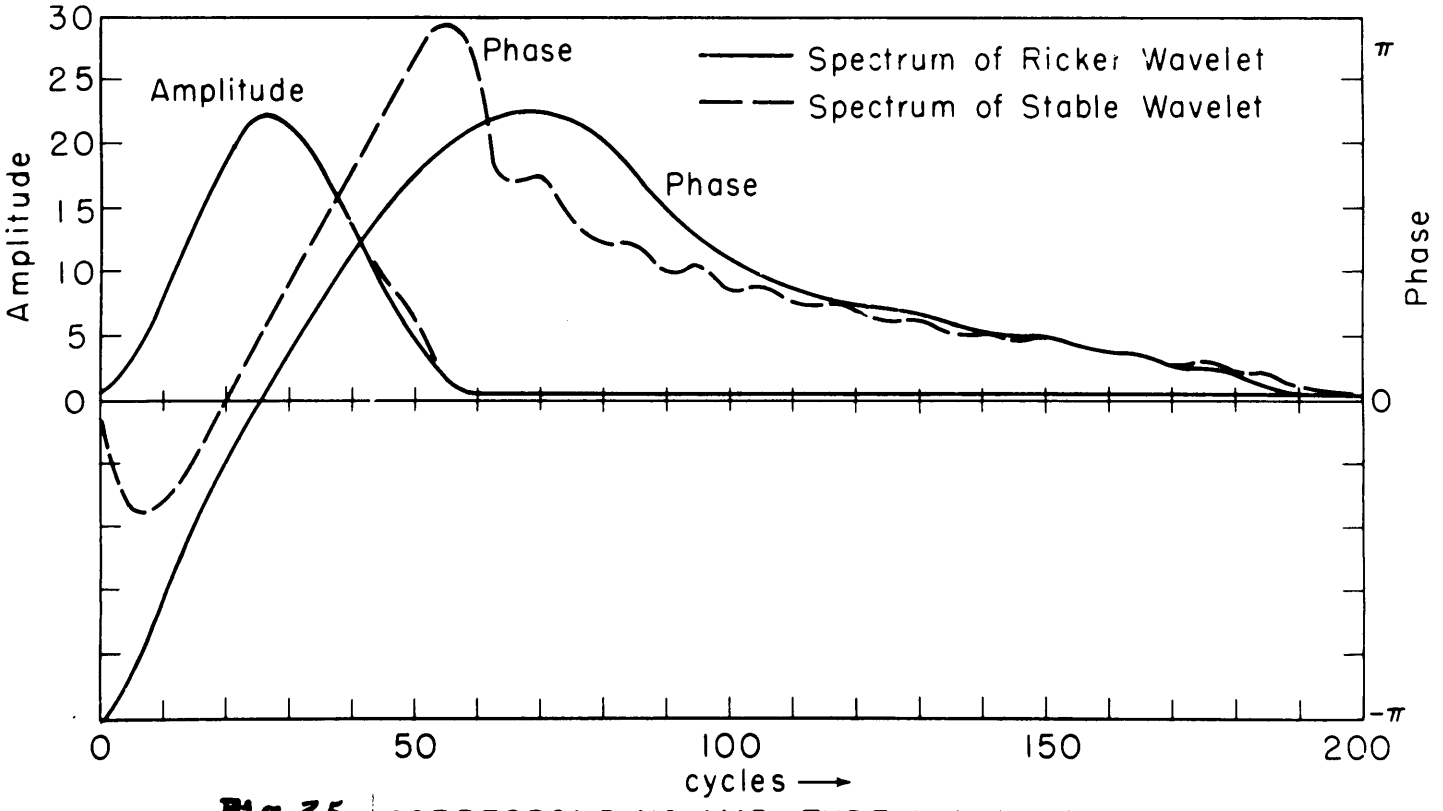

Fig.3.5 CORRESPONDING AMPLITUDE AND PHASE SPECTRA

belie this hypothesis (Fig. 3.6).

The modified inverse operator $\frac{1}{V(s)} - a(e^{bx}-1)$ and its spectral characteristics are shown in Figure 3.7. The spectral characteristics of the inverse of V(25), approximate fairly closely our conception of what the spectral characteristics of the best inverse operator should be--the amplitude spectra related reciprocally, and the phases, the negative of one another (Compare Fig. 3.1 and Fig. 3.7). The spectral characteristics of the inverse of $V(\infty)$, on the other hand do not approximate these desired features very closely.

Our definition of the most suitable operator for resolution implies that the result of convolving our operator V(s) with its modified inverse $\frac{1}{V(s)} - a(e^{bx}-1)$ should be a spike at the inception time of V(s), and that, there should be a minimum of energy after the spike. Figure 3.8 demonstrates the results of applying this criterion to our modified inverse operators. Both inverse operators give a spike at the time origin, and exhibit noise behind the spike as was to be expected from using approximations to the true inverse. However, the random noise content behind the spike for $V(\infty)$ is much larger than that for V(25), so large in fact that it precludes the possibility of using the modified inverse of $V(\infty)$ to resolve a wavelet complex in which random noise may be present.

As a test of the effectiveness of the inverse operator in resolving a wavelet complex, we consider a signal,

consisting of two wavelets of the V(25) type, of different amplitudes, separated by a time interval, and in which no noise is present. We operate upon them with the operator $\frac{1}{V(25)} - a(e^{bx}-1)$. Figure 3.9 illustrates the results of the convolution. In both examples, resolution is excellent with the spikes occurring at the inception times of the individual wavelets of the complex.

This success of our inverse operator as a resolver must be tempered with the realization that noise-free complexes of the form examined, rarely, if ever, occur in practice. Noise in the form of phasing and random energy is an inherent feature of every seismogram. Wavelet complexes, in which the individual wavelets are similar in shape, are the exception, rather than the rule. It is far more likely that the individual wavelets of a complex are dissimilar in shape, each representative of a reflection from a minor velocity discontinuity, at which there has been a change in the physical characteristics of the subsurface.

In view of this, the effects of these various factors on the contracting ability of our modified inverse operator were examined.

Figure 3.10 illustrates the effect of phasing in the ability of the inverse operator to produce a spike, when convolved with the original wavelet. Ideally, regardless of where the convolution process begins, at 1/4 h, 1/2 h, 3/4 h or 1 1/4 h (h is the spacing parameter, or the time interval between successive data points), the position of the spike,

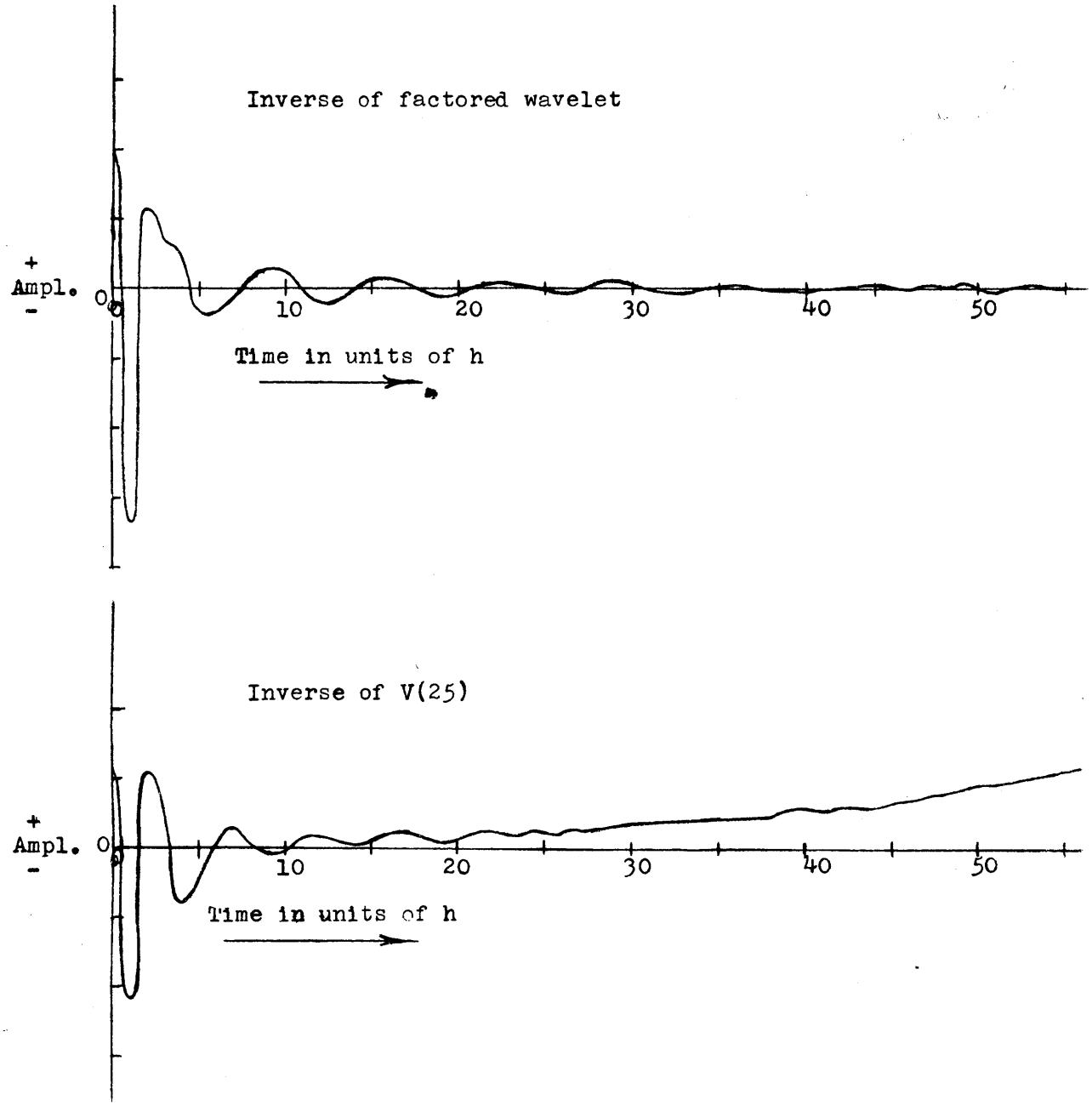

Fig. 3.6 COMPARISON OF $\frac{1}{V(25)}$ WITH THE INVERSE OF THE STABLE WAVELET ASSOCIATED WITH THE AMPLITUDE CHARACTERISTIC OF V(25)

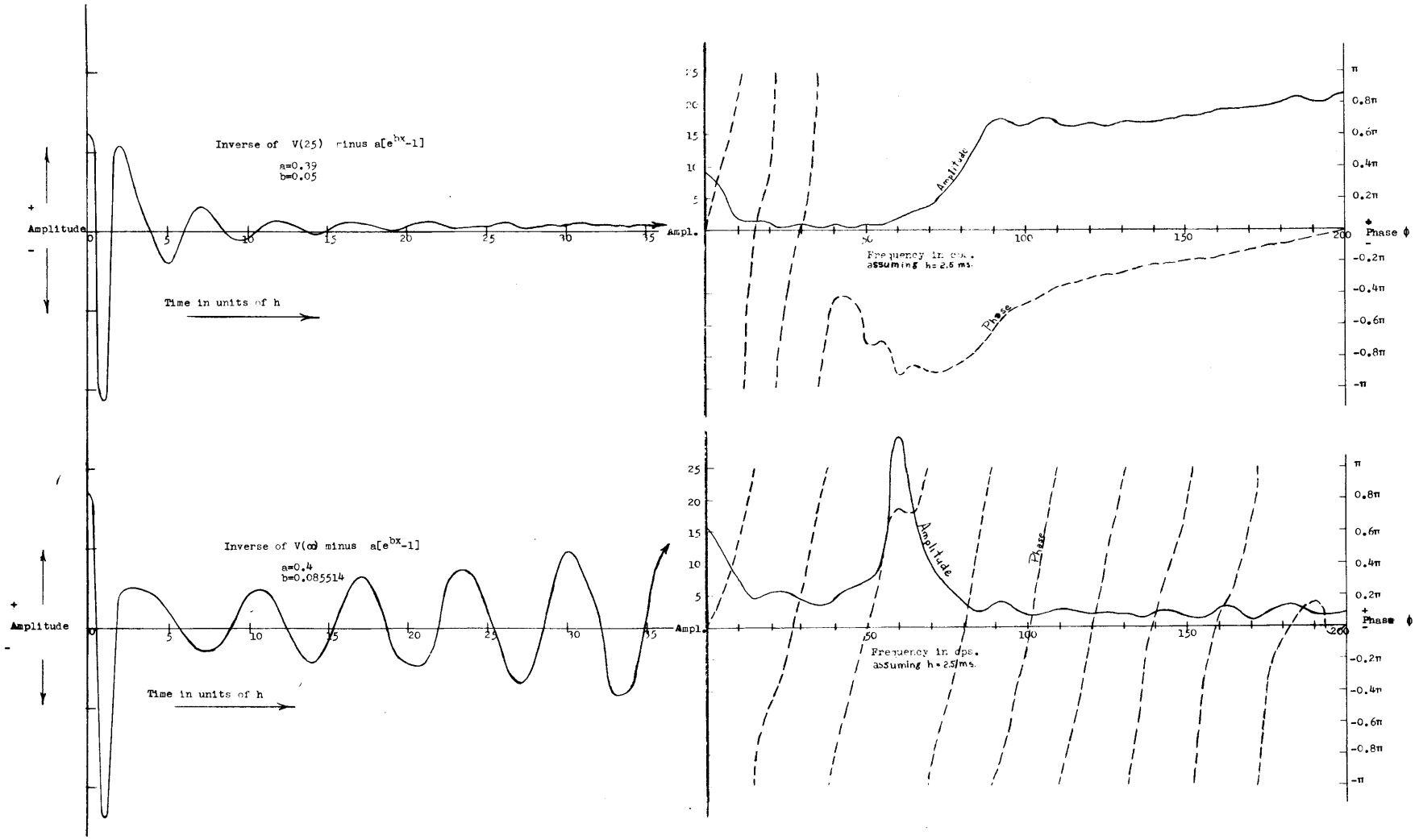

Fig. 3.7 Smoothed inverse operators and their spectral characteristics.

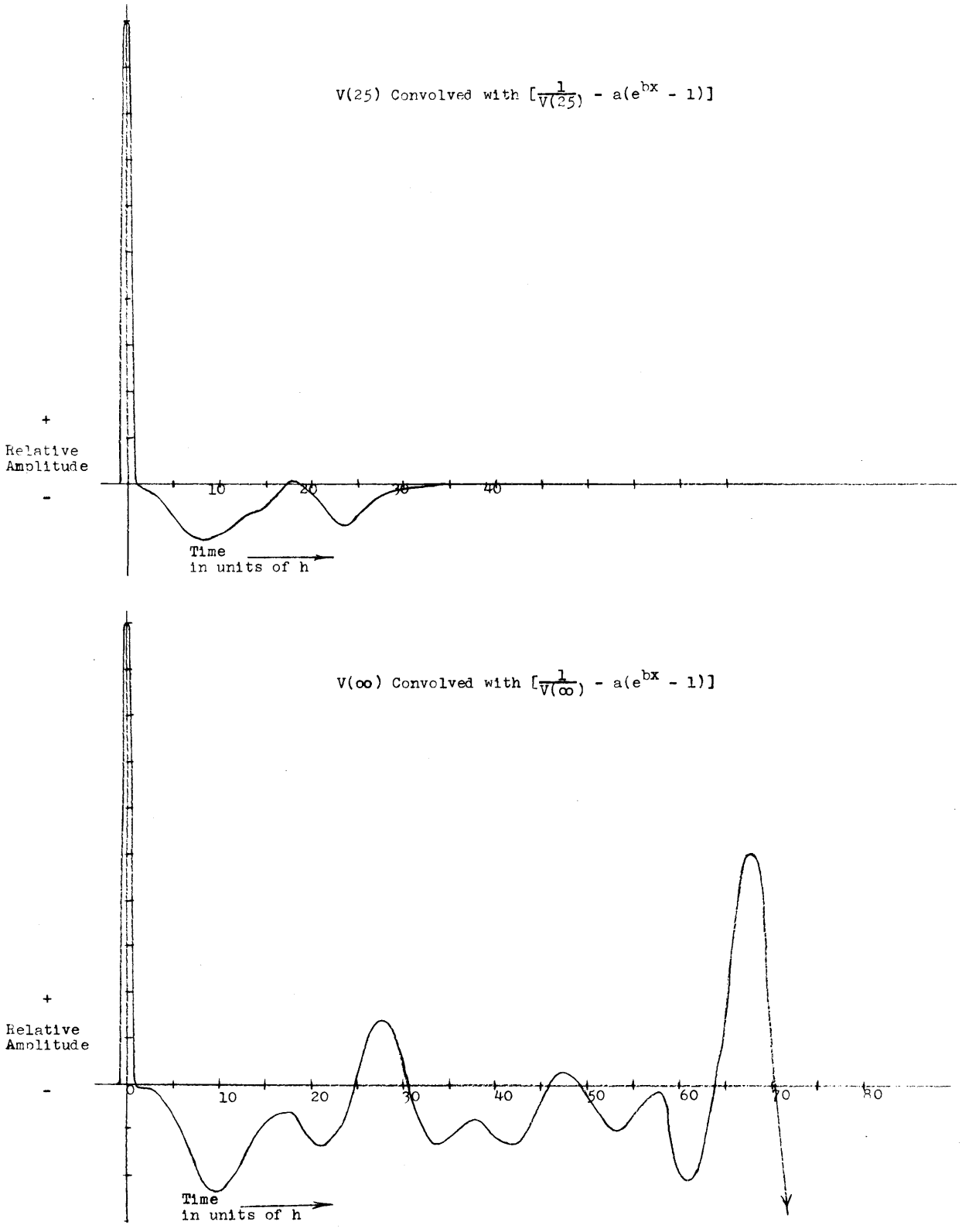

Fig. 3.8 Convolutions of V(25) and V(∞) with their approximate inverses

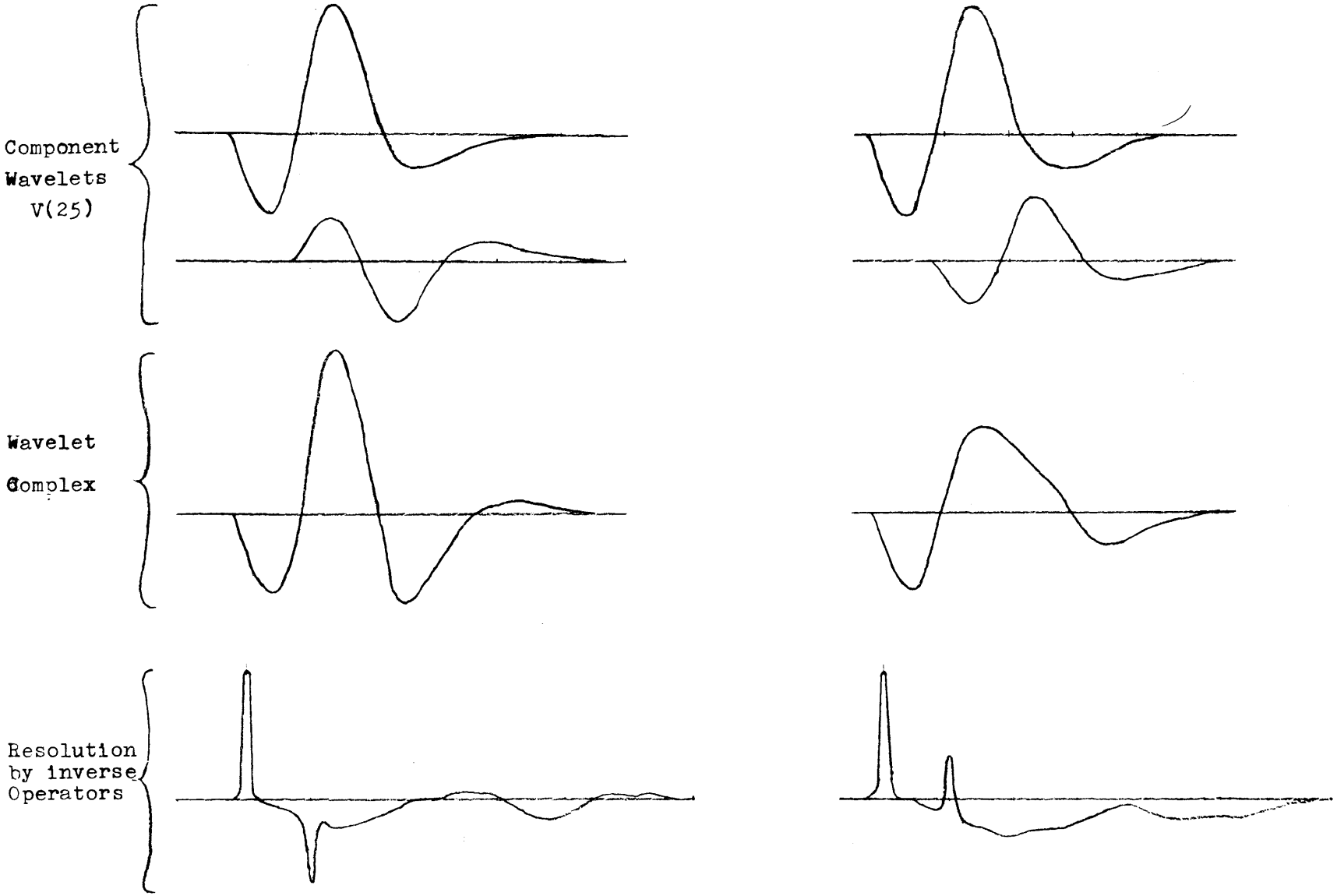

Fig. 3.9 Artificial wavelet complexes and their resolution by inverse operators

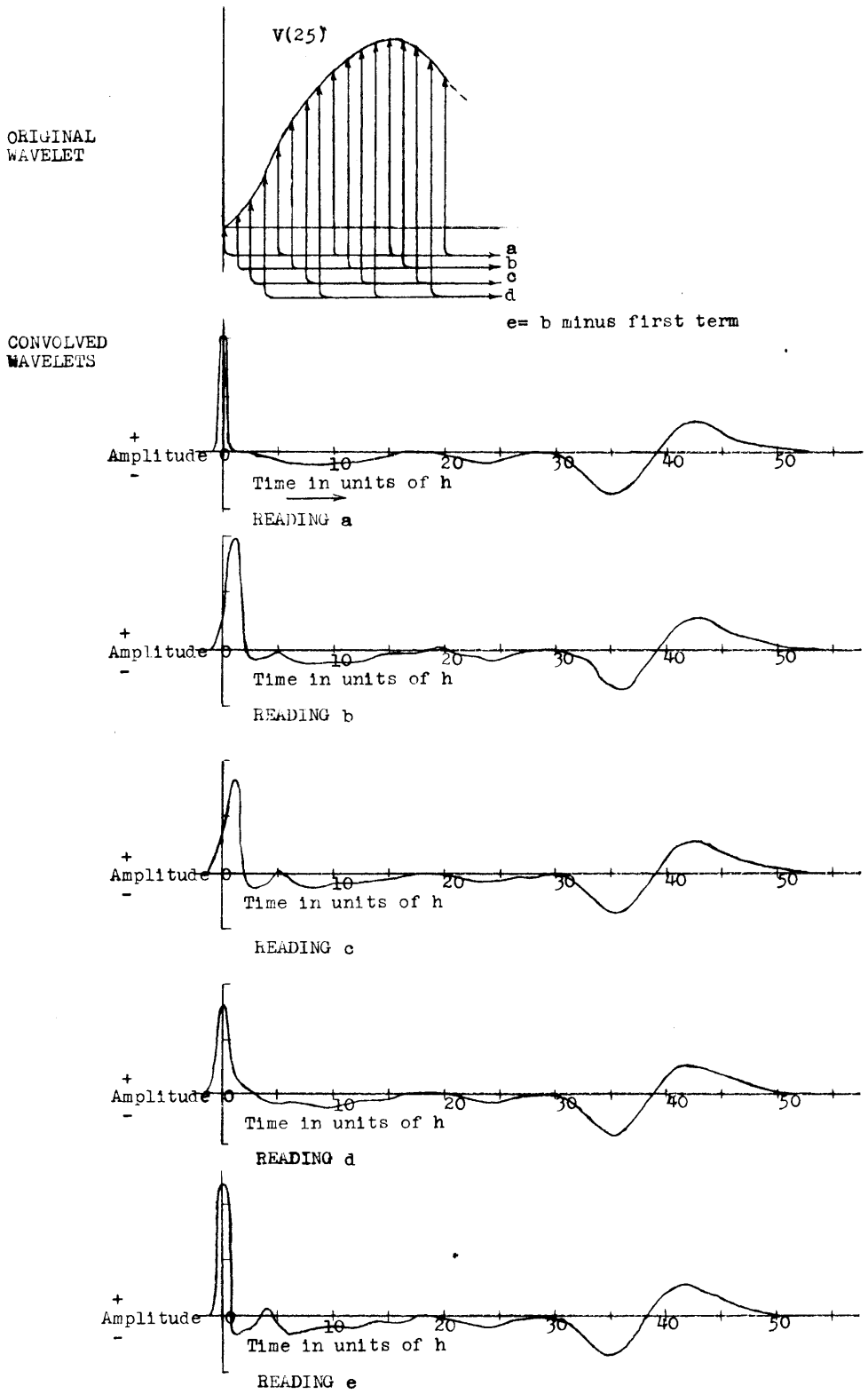

Fig. 3.10 Phasing test. Inverse operator of wavelet from readings (a) convolved with wavelets from readings in different phase relations

indicating the inception time of the wavelet, should not be altered. As can be seen from the figure there is a variation in the position of the spike, reaching a maximum at a phase shift of 1/2 h. However, the maximum displacement of the spike is at no time greater than 1 1/2 h, or, in time, approximately 4 milliseconds (h = 2.5 milliseconds). In terms of present day interpretative techniques, this represents a negligible error, especially if we recall that the arrival times of a reflection are in reality two-way times. Hence we may conclude that phasing has little effect on the contracting ability of our operator, although there is some evidence that the size of the spacing parameter h, relative to the wavelet length, may have an adverse affect. However, this can be easily remedied.

Figure 3.11 illustrates the effect of noise, in the form of alteration of wave-shape, upon our inverse operators. In this instance, we have convolved the modified inverse of V(25) with V(∞) and the modified inverse of V(∞) with V(25). At best, under such circumstances, we would like some indication of the arrival time of the wavelet, and a minimum of noise after such an indication. The modified inverse operator of V(∞) lacks all of the desirable characteristics, for the results of convolving this inverse with V(25) gives no discernible indication of the arrival time of V(25), and exhibits a highly divergent tail, which would make resolution of a later wavelet in a complex virtually impossible. On

the other hand, the result of convolving the modified inverse of V(25) with V(∞) does exhibit a spike at the arrival time of V(∞), but once more the noise level following the spike is quite high, although not as excessive as for the inverse operator of V(∞).

These results indicate that both inverse operators are sensitive to noise in the form of variation in wave-shape. However, it should be pointed out that the wave-shapes of V(∞) and V(25), with which this experiment was conducted, are quite diverse in character (Fig. 3.1), and, although such wide variations in wave-form can appear in a real seismic complex, it is more probable that the variation in the shape of the individual components of such a complex is less abrupt, and hence the effect of such variations less important in the resolving ability of the inverse linear operator.

In summary, we may say that the inverse operator $\frac{1}{V(s)} - a(e^{bx}-1)$ is a suitable resolver in the noise-free case, for the type of wavelets considered, but its effectiveness in the presence of noise must be considered in the light of the reservations enumerated above.

Unfortunately, as noted in the introduction, the Ricker wavelets are a poor representation of the seismic reflections observed in reality, and as a consequence, the experimental methods used here in deriving the resolving operator can only serve as a guide in the derivation of suitable operators for a real reflection complex.

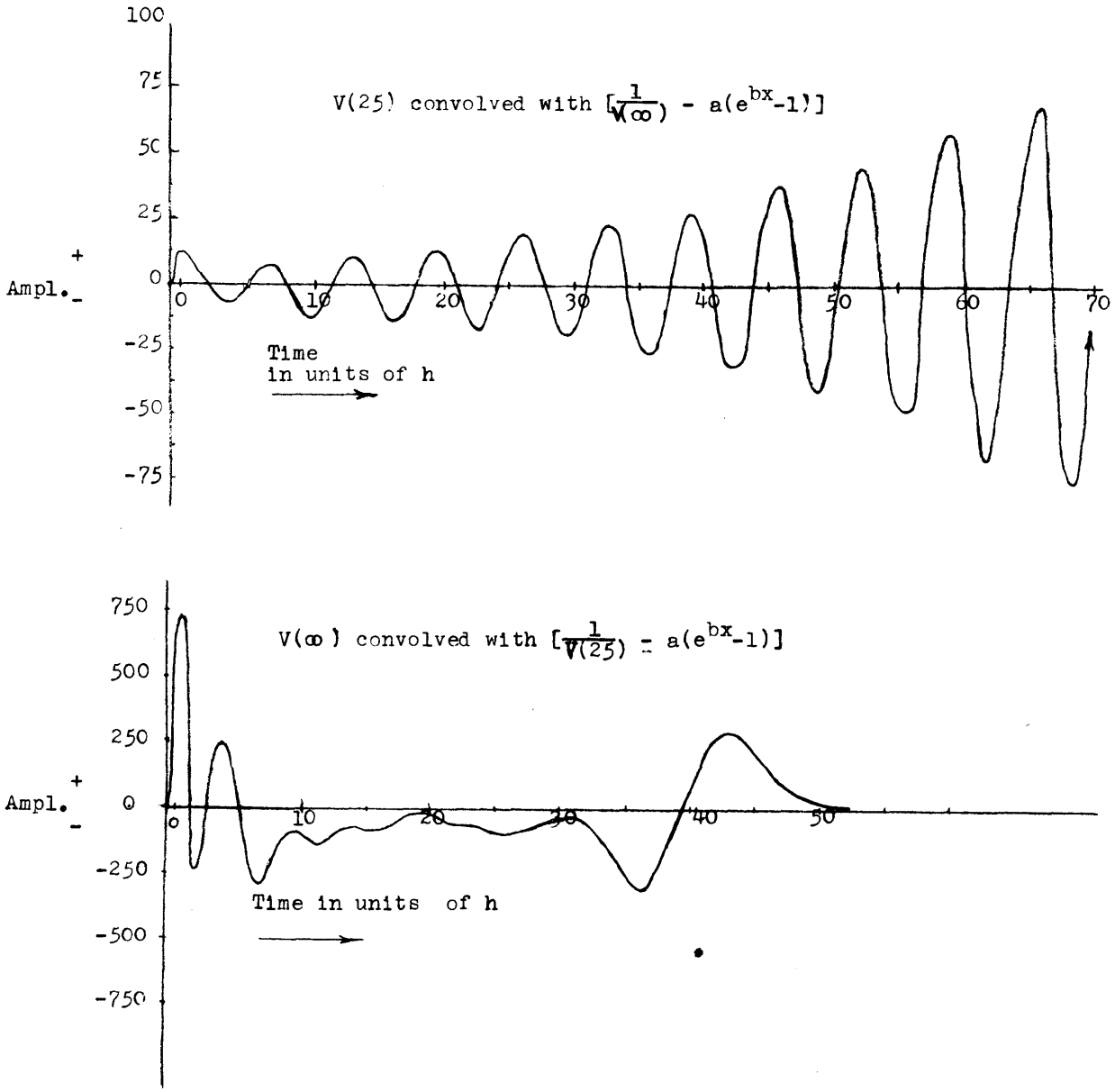

Fig. 3.11 Results of convolving approximate inverses of V(25) and V(∞) with V(∞) and V(25) respectively.

III.5. The Contractor Operator for a Real Reflection Complex

The reflection complex examined was obtained from a suite of records supplied by the Atlantic Refining Company. These records exhibit thinning between events A and B, which may be indicative of a stratigraphic pinch-out. (Fig. 3.12). Reflections A and B, which appear as two distinct events at approximately 0.98 and 1.07 seconds on record 7.19, have apparently coalesced into one complex reflection on record 7.16.

Our objective was to obtain an operator with which the noise or undesirable signal, represented by event A, could be contracted to a spike at the arrival time of event A, with a minimum of energy behind this spike, and thus permit an accurate determination of the arrival time of event B, throughout the suite of records.

A typical wavelet of the event A was obtained from record 7.19 by averaging the digitalized form of the wavelet over every other trace of the record. This average wavelet was then modified so as to have a tail whose amplitude approaches zero smoothly, and a zero time origin. Figure 3.13 illustrates this average wavelet and its spectral characteristics.

The inverse of this average wavelet was then calculated, and, in contrast to the inverse of the Ricker wavelet, it was highly divergent, without any recognizable pattern (Fig. 3.14). Consequently, no technique was available for increasing the useable length of the inverse operator, and the inverse truncated to the first nine terms appears to be the only

7.19 7.18 7.17 7.16

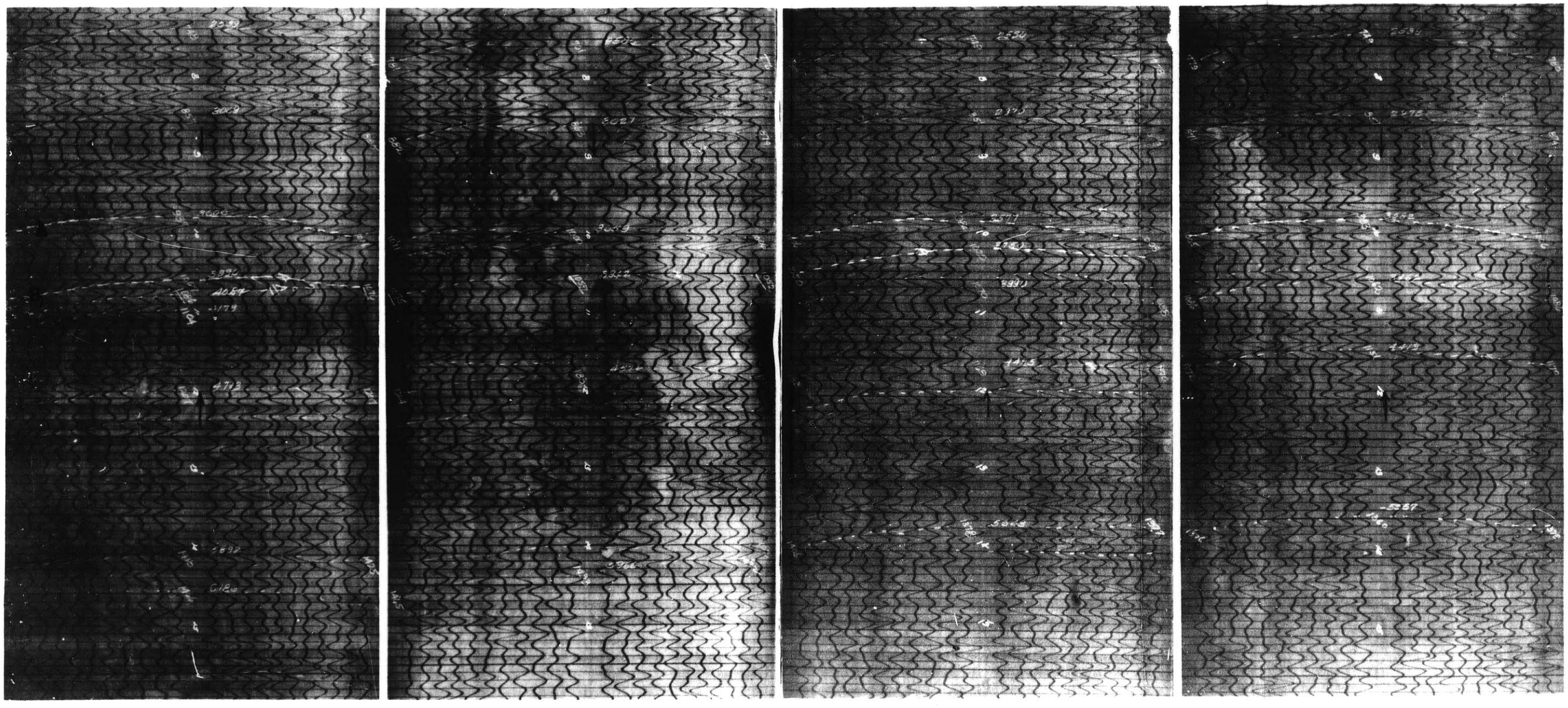

Fig. 3.12 Four records of the Atlantic Refining Co. exhibiting pinchout.

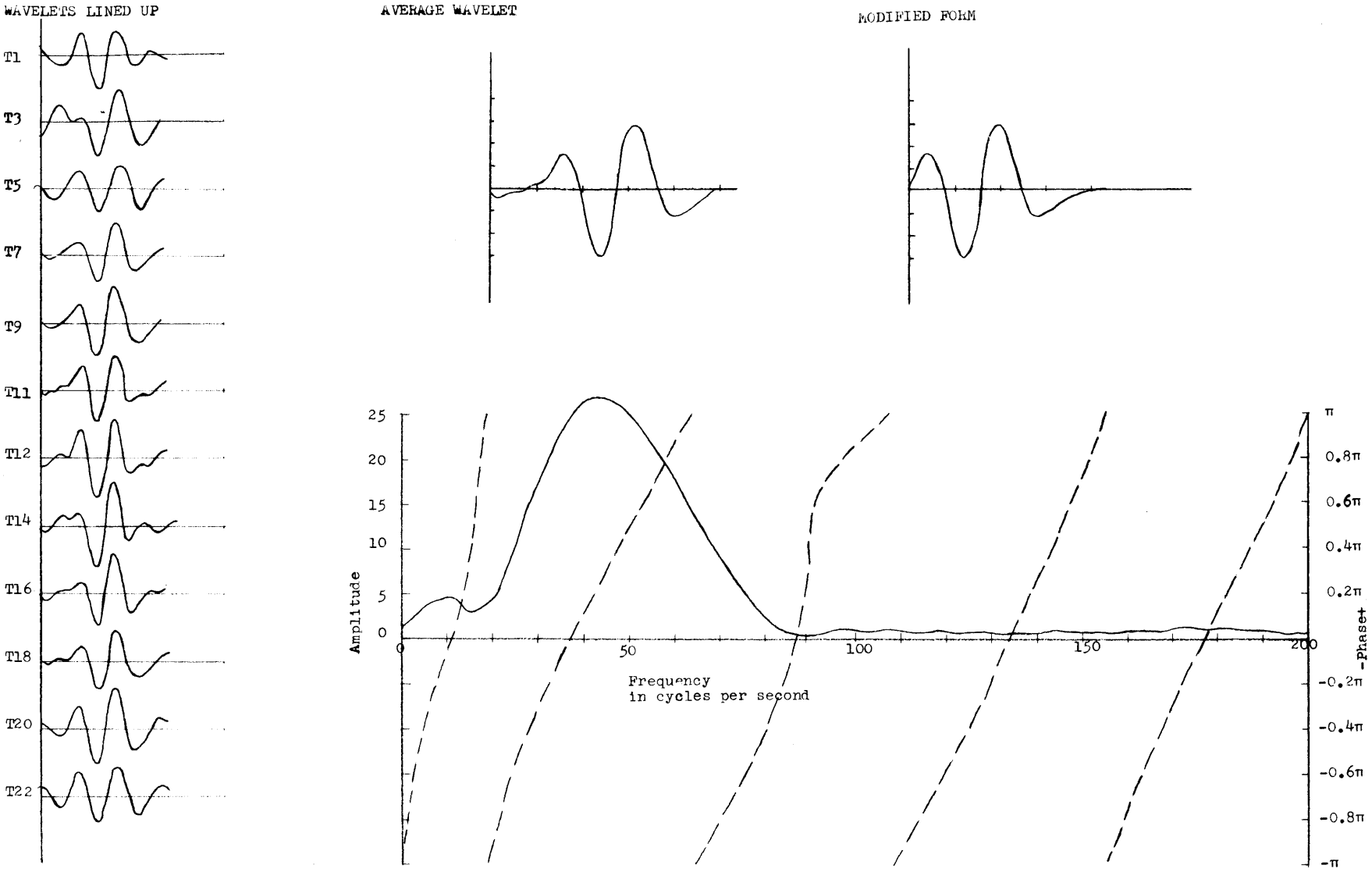

Fig. 3.13 The average wavelet from 7.19 and its spectral characteristics

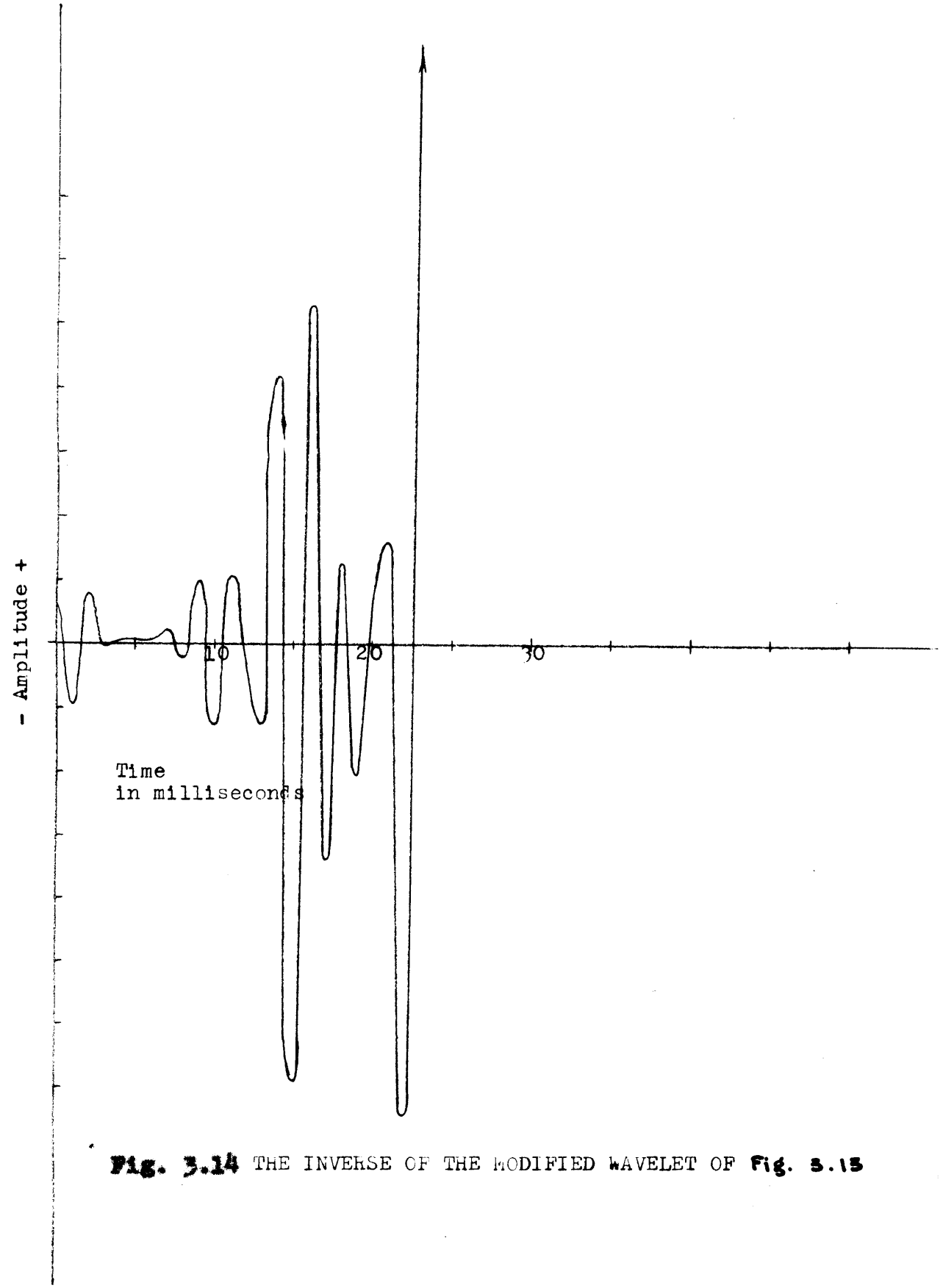

Fig. 3.14 THE INVERSE OF THE MODIFIED WAVELET OF **Fig. 3.13**

practicable operator derivable directly from the exact inverse.

This nine-term operator should give resolution over a time interval of twenty milliseconds (in terms of our spacing parameter h,—8 h). However, its short length would preclude the possibility of using it for resolving events A and B over an extensive range.

As a test of the resolving ability of such an operator, a noise-free complex signal was operated upon by the nine-term inverse. The signal consisted of the superposition of the average wavelet of event A, and an average wavelet representative of event B on record 7.19 (obtained in a similar fashion to that of event A), which lagged A by ten milliseconds (4 h). Figure 3.15 illustrates the result of this convolution. Spikes occur at the inception times of both events A and B, in spite of the difference in wave-shape between the two wavelets. However, it must be pointed out that this is once again a noise-free situation, and the effects of noise, particularly in an operator of such short length, may well inhibit its usefulness as a resolver, even in those optimum cases, when the reflections may be separated by an interval of less than twenty milliseconds.

The effects of random noise and a wide separation of events are illustrated in Figure 3.16, which demonstrates the result of convolving the operator with several digitalized traces of record 7.19. It is doubtful whether any sort of coherent picture of the relationship between events A and B can be obtained. Evidently the presence of noise and the

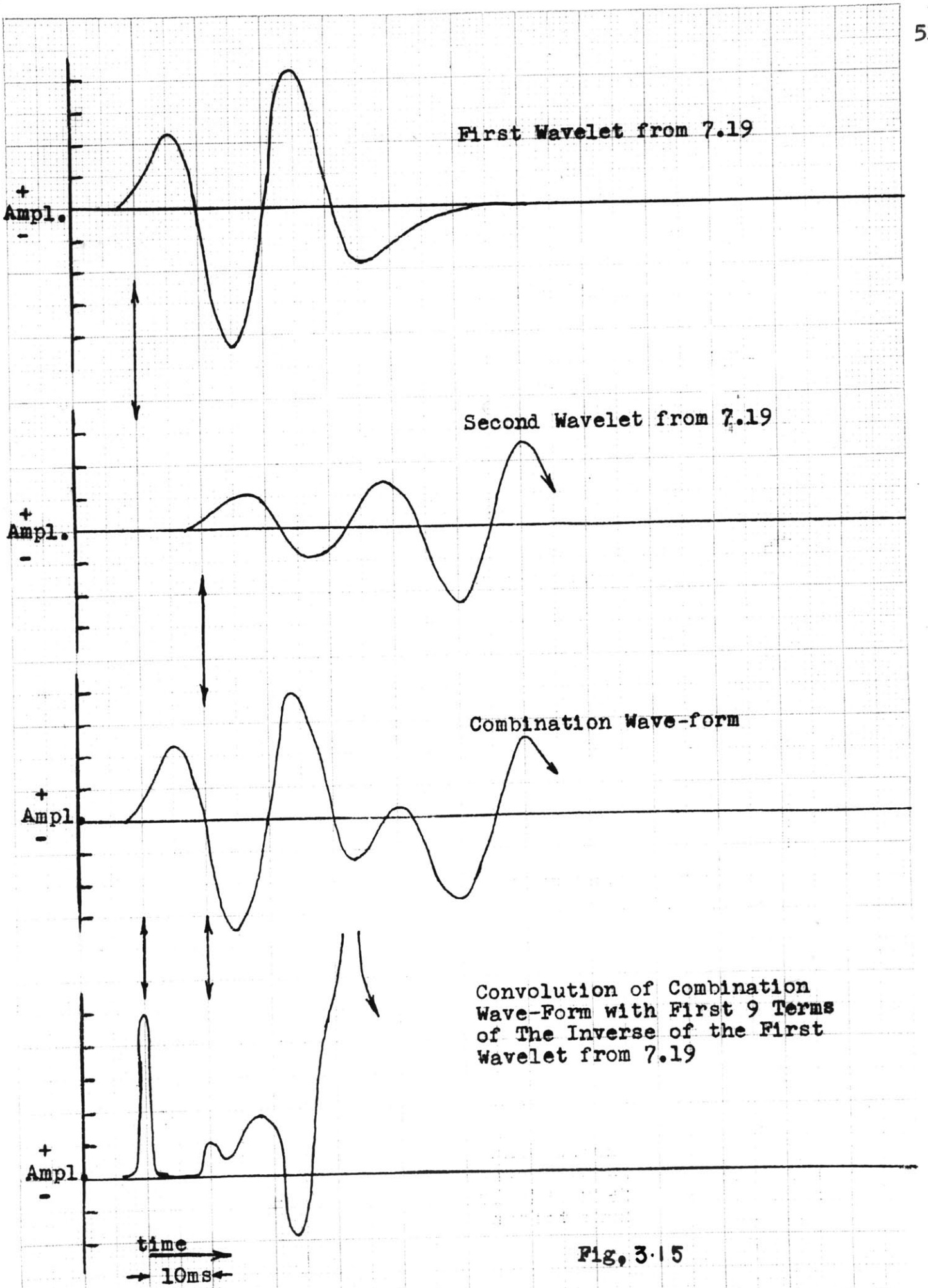
First Wavelet from 7.19
+
Ampl.
-
Second Wavelet from 7.19
+
Ampl.
-
Combination Wave-form
+
Ampl
-
Convolution of Combination Wave-Form with First 9 Terms of The Inverse of the First Wavelet from 7.19
+
Ampl
-
time
10ms

Fig. 3·15

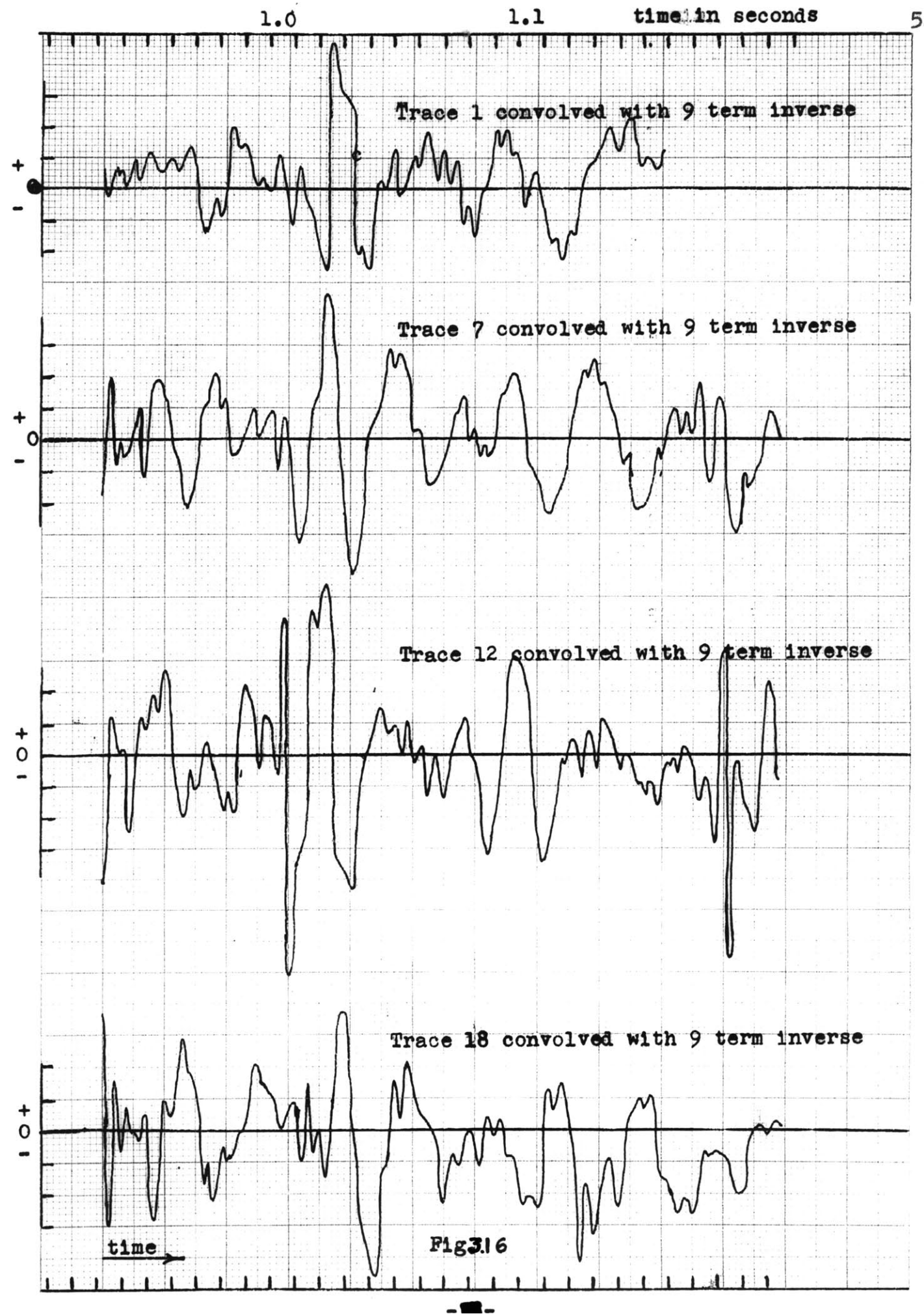
1.0
1.1
time in seconds
Trace 1 convolved with 9 term inverse
Trace 7 convolved with 9 term inverse
Trace 12 convolved with 9 term inverse
Trace 18 convolved with 9 term inverse
+
-
0
time

Fig3.16

separation of the events A and B by a time interval of approximately ninety milliseconds makes resolution virtually impossible.

An attempt to approximate the average wavelet of event A, by the Ricker wavelet V(∞), and thus use its modified inverse as a contractor proved abortive. Convolution of such an inverse with the average wavelet of event A, produced a series of divergent terms and no recognizable spike.

Ideally, as stated above, to obtain a white light spectrum upon convolution, inverse operator should exhibit spectral characteristics inverse to those of the original operator or wavelet. The spectrum of this inverse operator may be expressed as a power series (equation 3.3.2), and the Fourier cosine transform of such a series, should thus be the representation in the time domaine of the inverse operator. A symmetric operator, which may be less sensitive to noise is obtained by unfolding (computing the image of the function with respect to the amplitude axis) this cosine transform.

Figures 3.17 and 3.18 illustrate the symmetric operators and their amplitude spectra, obtained in the above manner for the average wavelet of event A, modified to exhibit a large initial term (sharp-front wavelet), and also modified to start with gradually increasing amplitude (smoothed wavelet).

Figures 3.19, 3.20 and 3.21 illustrate the results of convolving such symmetric operator of various lengths with these modified wavelets. A doublet spike is obtained in each

instance. However, the amplitude of the extraneous signal, preceding and following this spike, appears to be an inverse function of the operator length. The operator containing only fifteen terms has a very low ratio of spike amplitude to extraneous signal amplitude.

In an effort to improve this ratio, and thus the resolution of reflections in the presence of noise, the operator was smoothed by weighting its coefficients, according to the method of Cesarc sums. The result of convolving the smoothed symmetric operator, derived from a sharp-front wavelet, and the smoothed average wavelet of event A is shown in Figure 3.22, for various lengths of operator. There is little improvement in this ratio, and what is perhaps wholly condemnatory, the doublet spike, representing the contraction of the wavelet, is no longer well-defined.

As a test of the effectiveness of the symmetric operator (unsmoothed) in resolving reflections in the presence of noise, the twenty-five term operator, derived from the smoothed wavelet, and the forty-nine term operator derived from the sharp-front wavelet, were convolved with the digitalized traces of record 7.19 over the interval from 0.91 seconds to 1.16 seconds. The results of these convolutions are shown in Figures 3.23 and 3.24 respectively. There appears to be little distinction between the effectiveness of the twenty-five term or of the forty-nine term operator. Although the presence of event A, in the form of a spike, can be seen on practically all traces, event B, at approximately 1.07

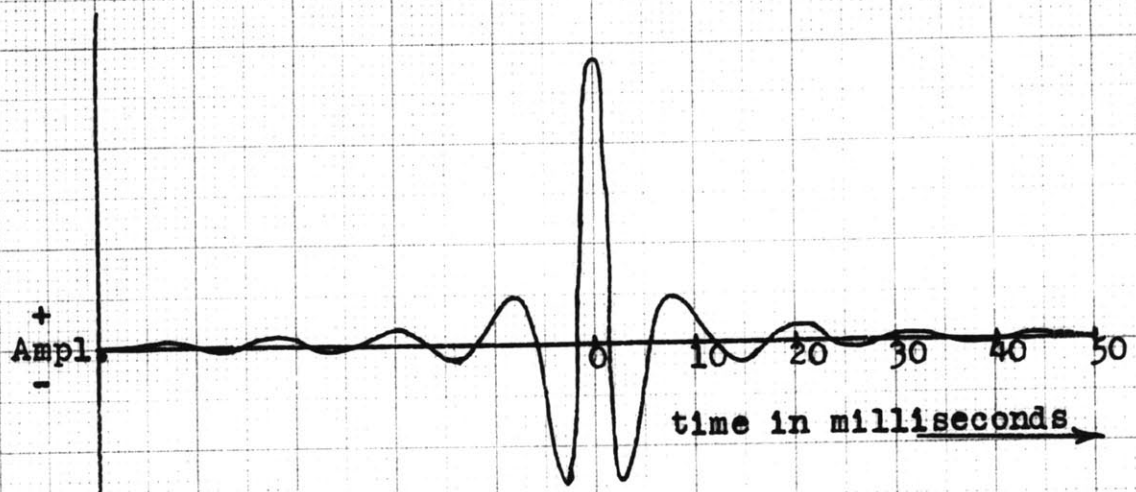

SYMMETRIC OPERATOR FOR SMOOTHED WAVELET FROM 7.19

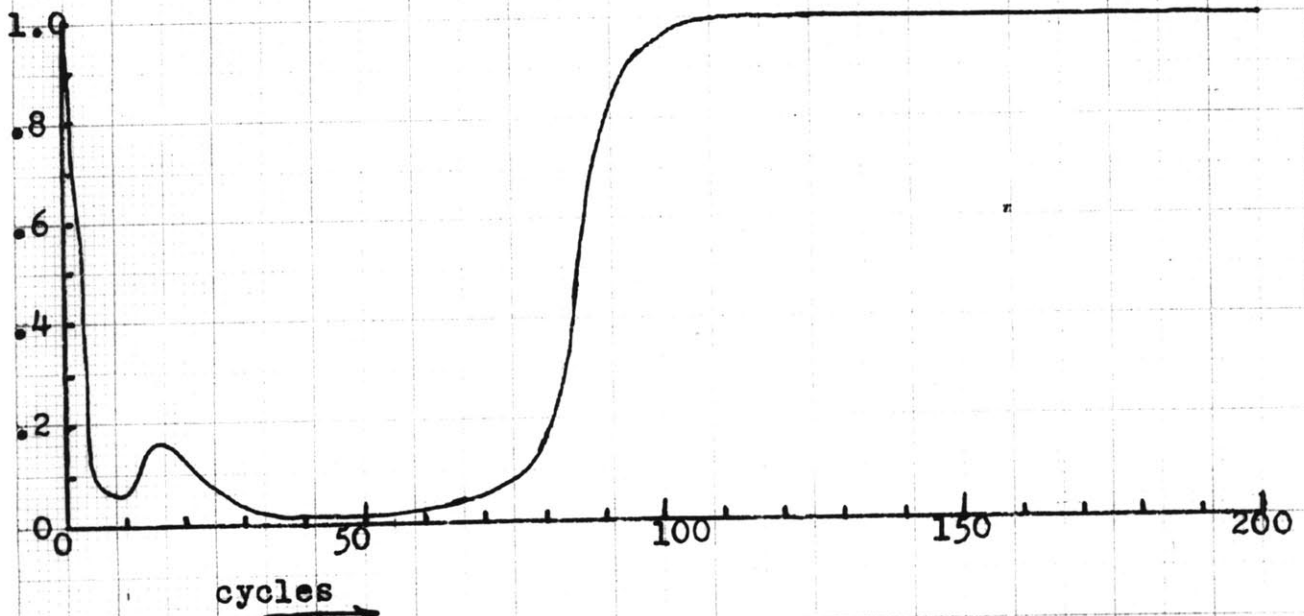

RECIPROCAL OF AMPLITUDE SPECTRUM OF SMOOTHED WAVELET FROM7.19

Fig 3.7

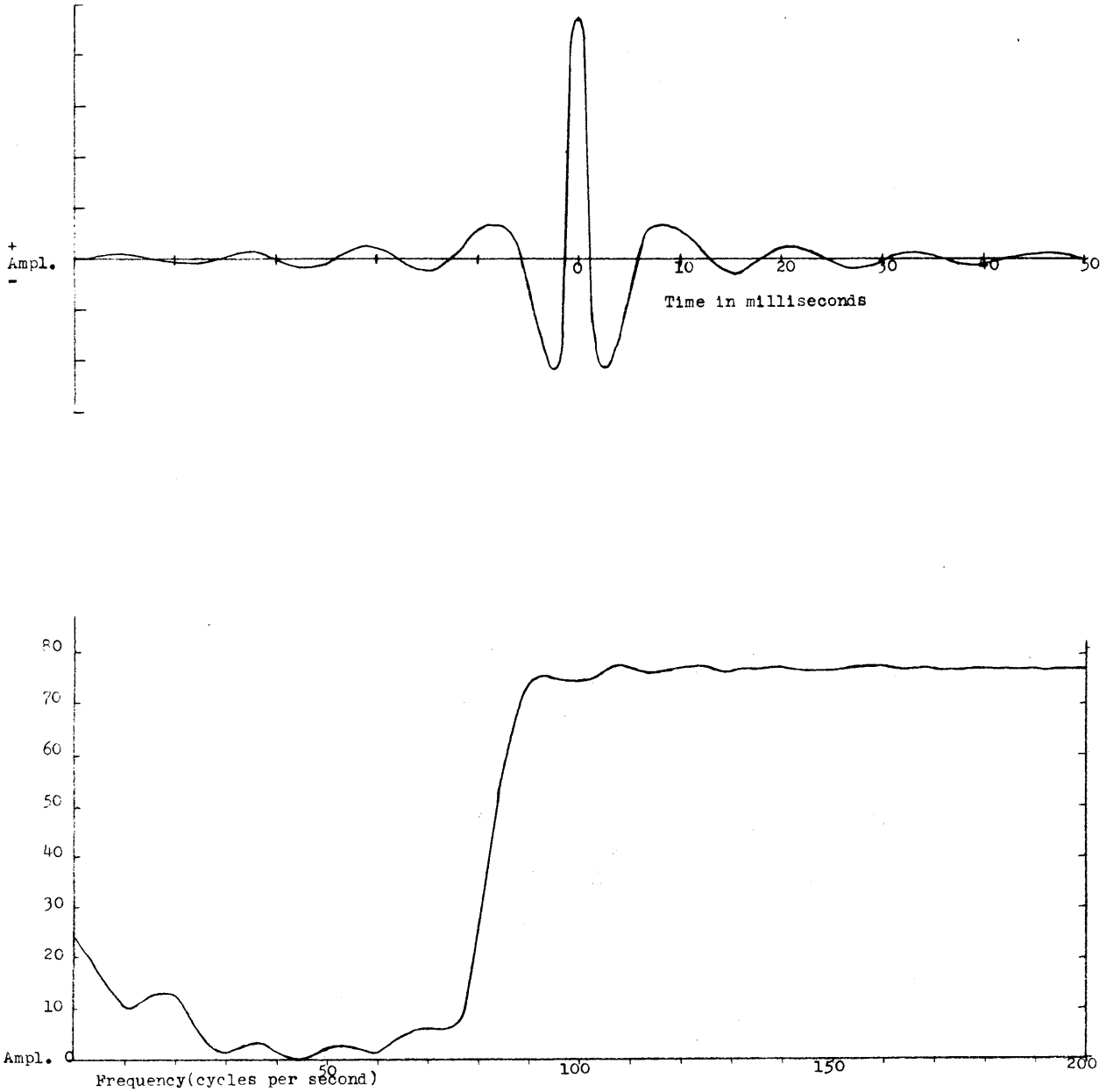

Fig. 3.18 Symmetric operator and its amplitude characteristics obtained from cosine transform of reciprocal of amplitude characteristic of Fig. 3.12.

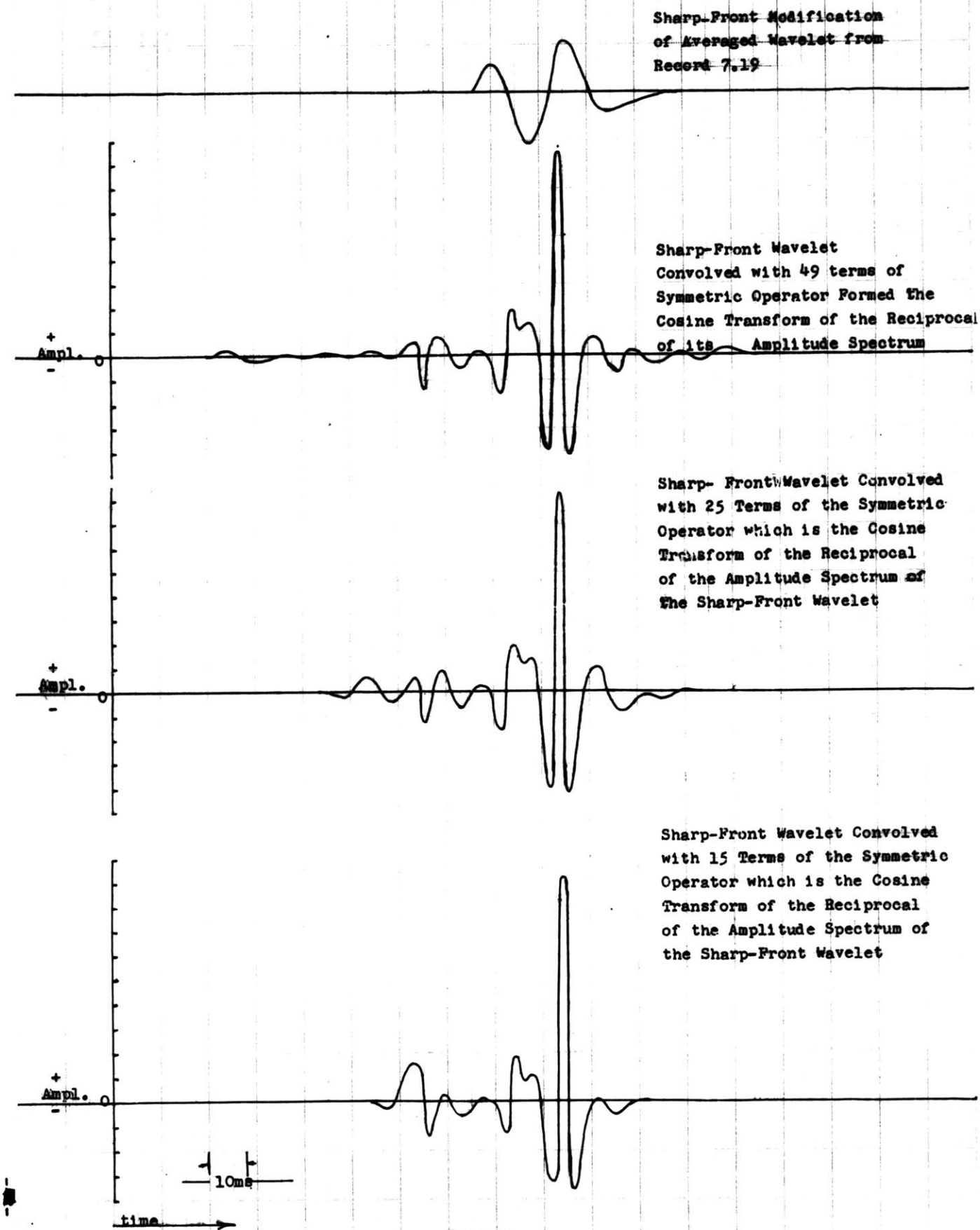
Sharp-Front Modification of Averaged Wavelet from Record 7.19
Sharp-Front Wavelet Convolved with 49 terms of Symmetric Operator Formed the Cosine Transform of the Reciprocal of its Amplitude Spectrum
+
Ampl.
-
0
Sharp- FrontWavelet Convolved with 25 Terms of the Symmetric Operator which is the Cosine Transform of the Reciprocal of the Amplitude Spectrum of the Sharp-Front Wavelet
+
Ampl.
-
0
Sharp-Front Wavelet Convolved with 15 Terms of the Symmetric Operator which is the Cosine Transform of the Reciprocal of the Amplitude Spectrum of the Sharp-Front Wavelet
+
Ampl.
-
0
10ms
time

Fig.3-19

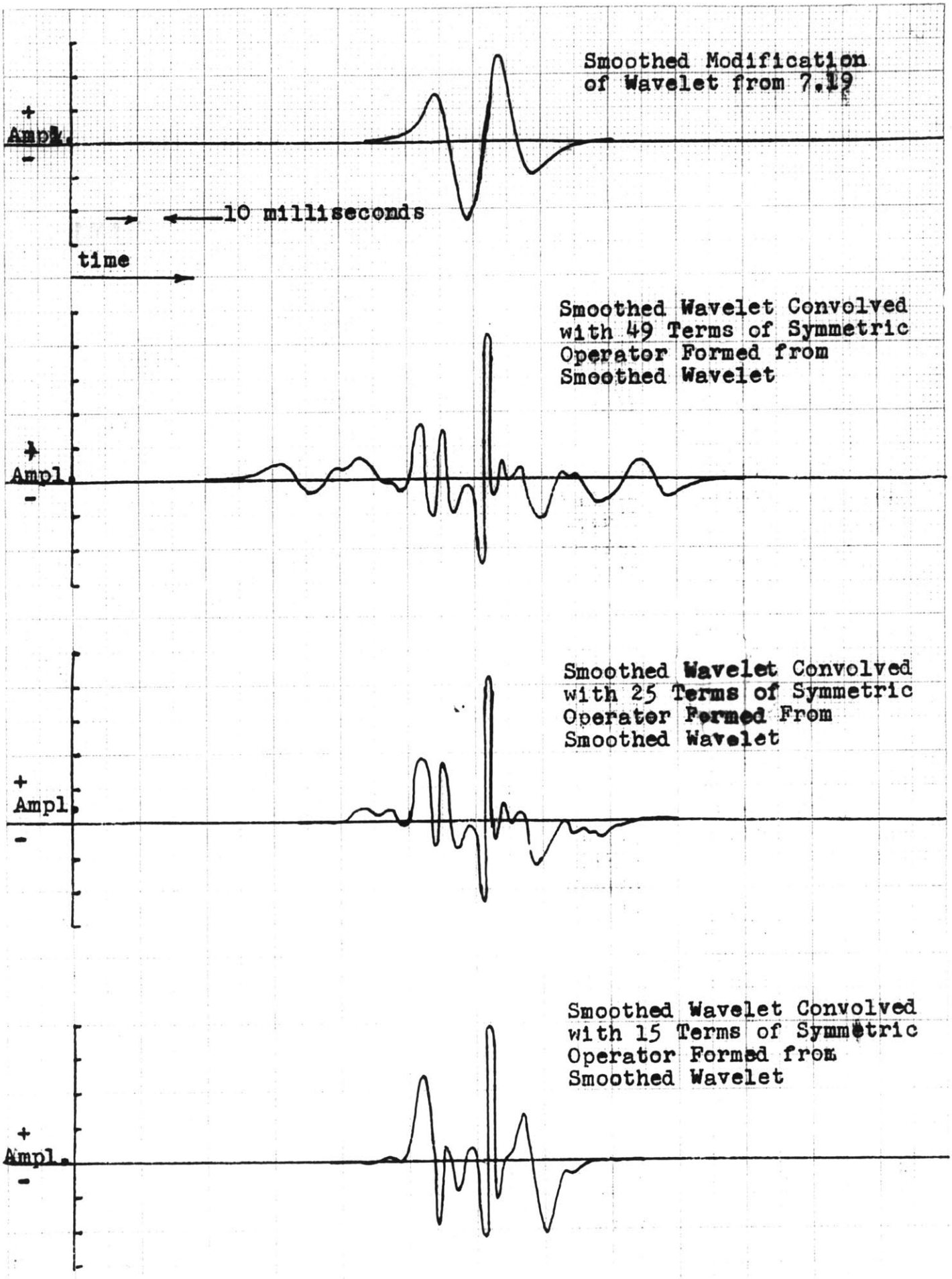
Smoothed Modification of Wavelet from 7.19
+
Ampl.
-
10 milliseconds
time
Smoothed Wavelet Convolved with 49 Terms of Symmetric Operator Formed from Smoothed Wavelet
+
Ampl.
-
Smoothed Wavelet Convolved with 25 Terms of Symmetric Operator Formed From Smoothed Wavelet
+
Ampl.
-
Smoothed Wavelet Convolved with 15 Terms of Symmetric Operator Formed from Smoothed Wavelet
+
Ampl.
-

Fig.320

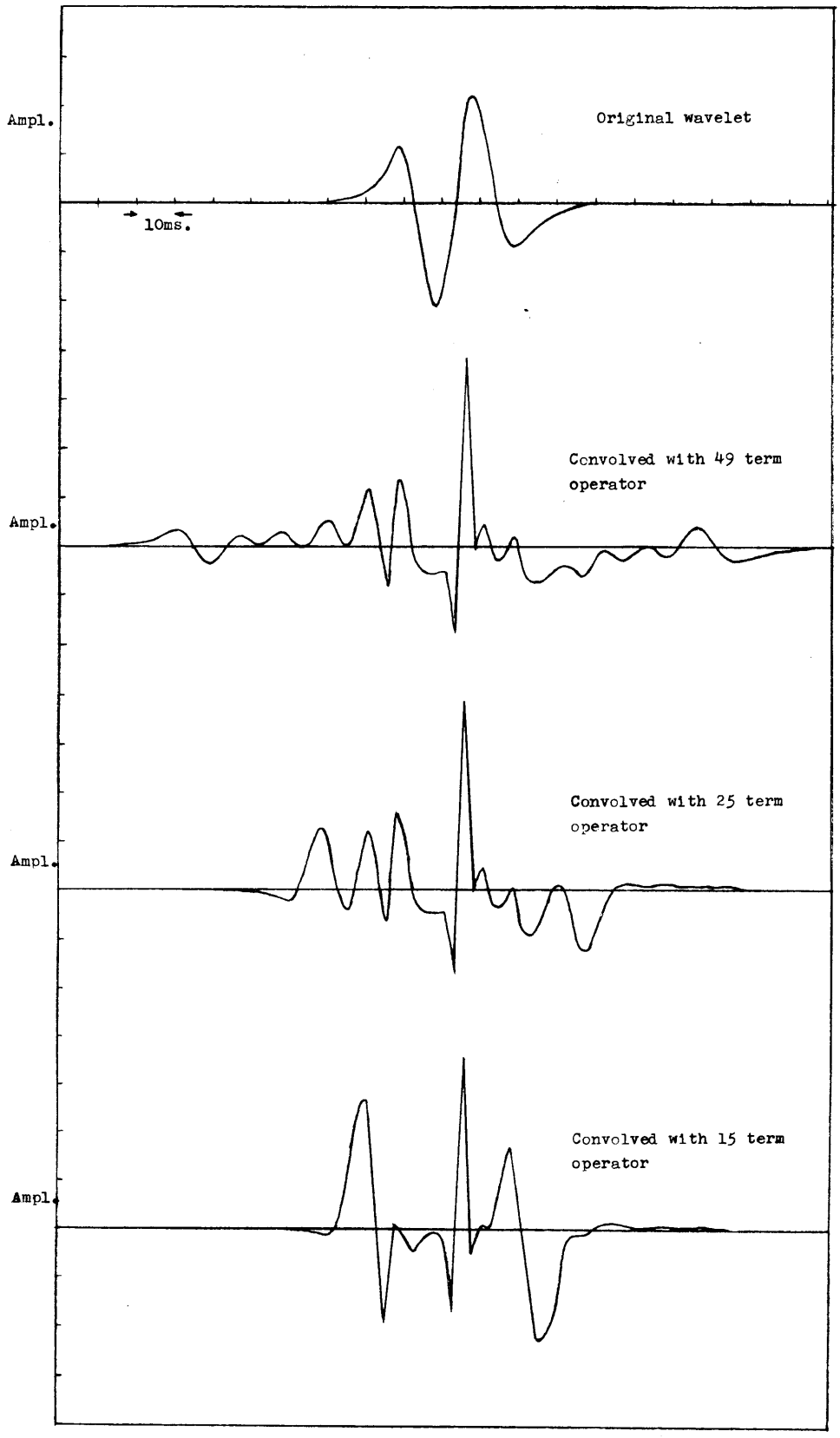

Fig. 3.21 Convolutions of wavelet of Fig. 3.12 with symmetric operators of various lengths.

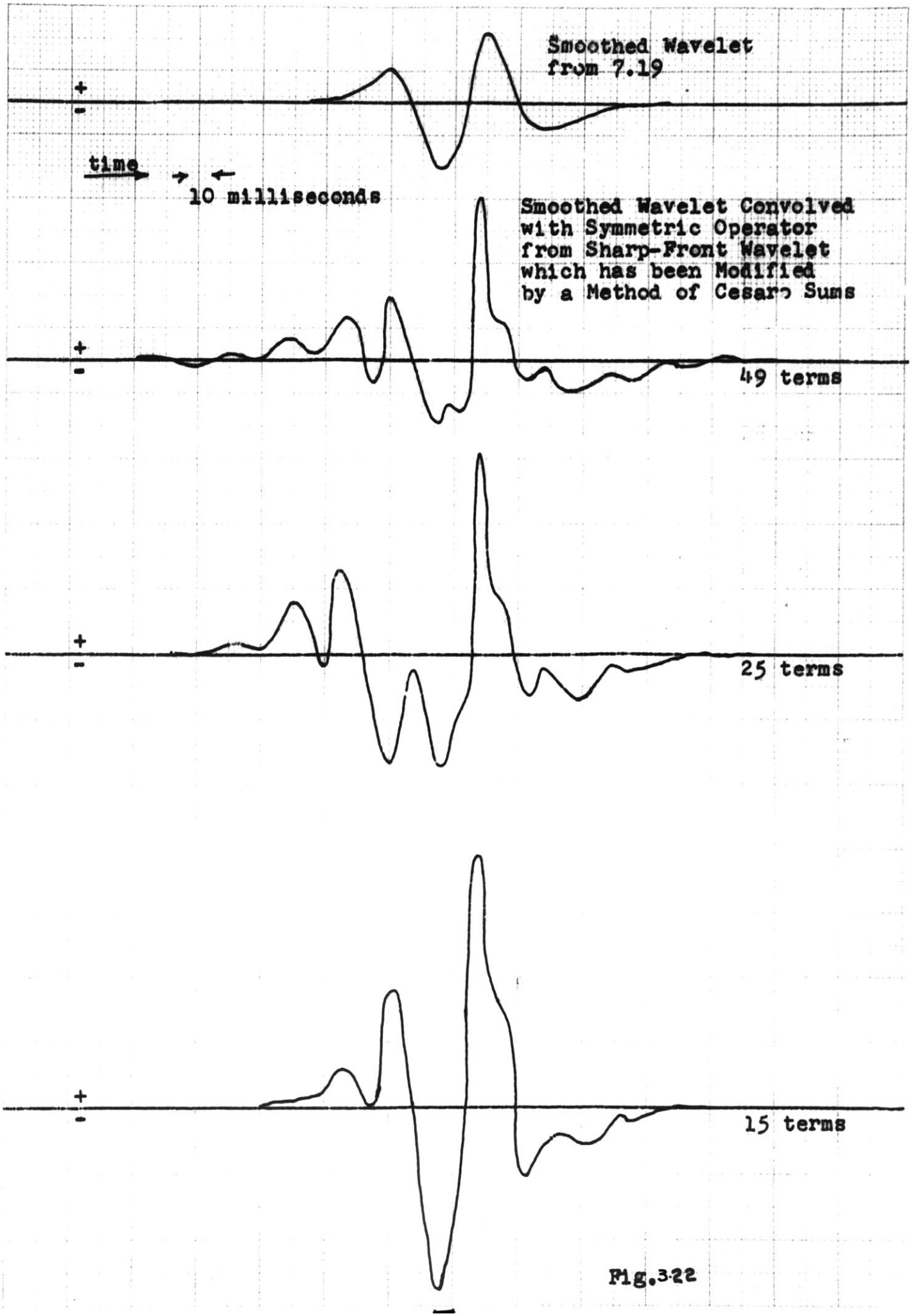
Smoothed Wavelet
from 7.19
+
-
time
10 milliseconds
Smoothed Wavelet Convolved
with Symmetric Operator
from Sharp-Front Wavelet
which has been Modified
by a Method of Cesaro Sums
+
-
49 terms
+
-
25 terms
+
-
15 terms

Fig.3.22

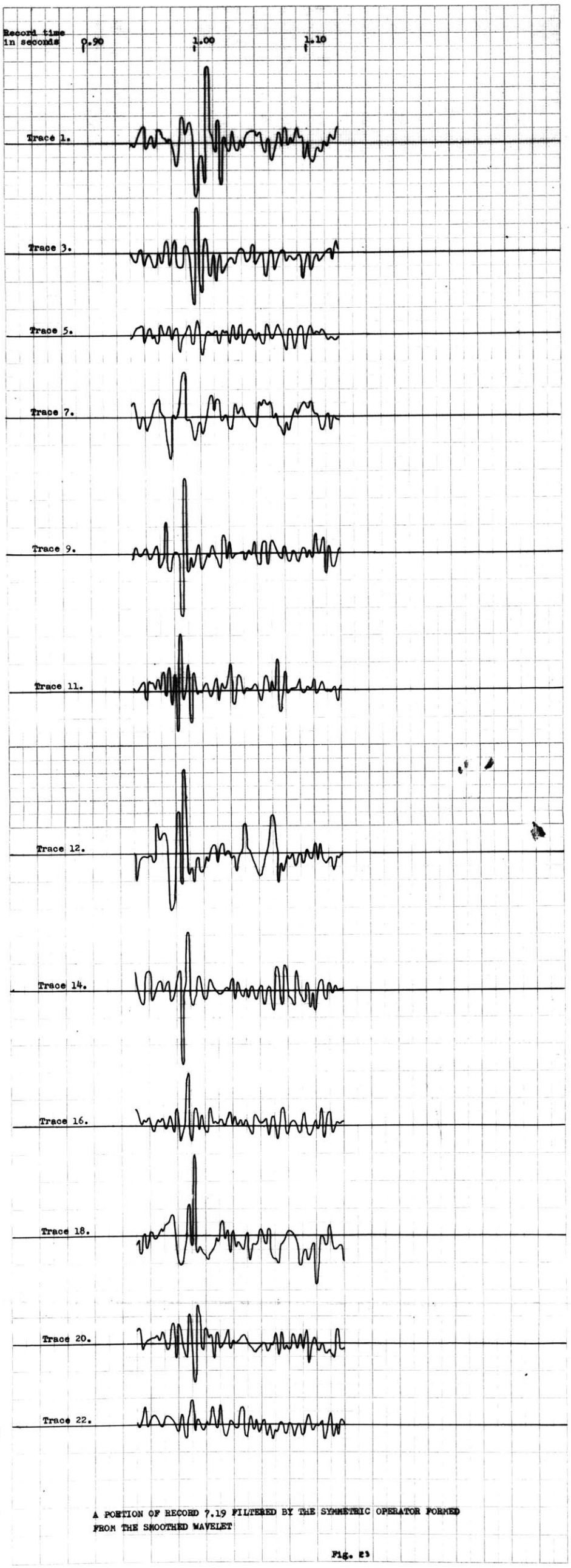

A PORTION OF RECORD 7.19 FILTERED BY THE SYMMETRIC OPERATOR FORMED FROM THE SMOOTHED WAVELET

Fig. 23

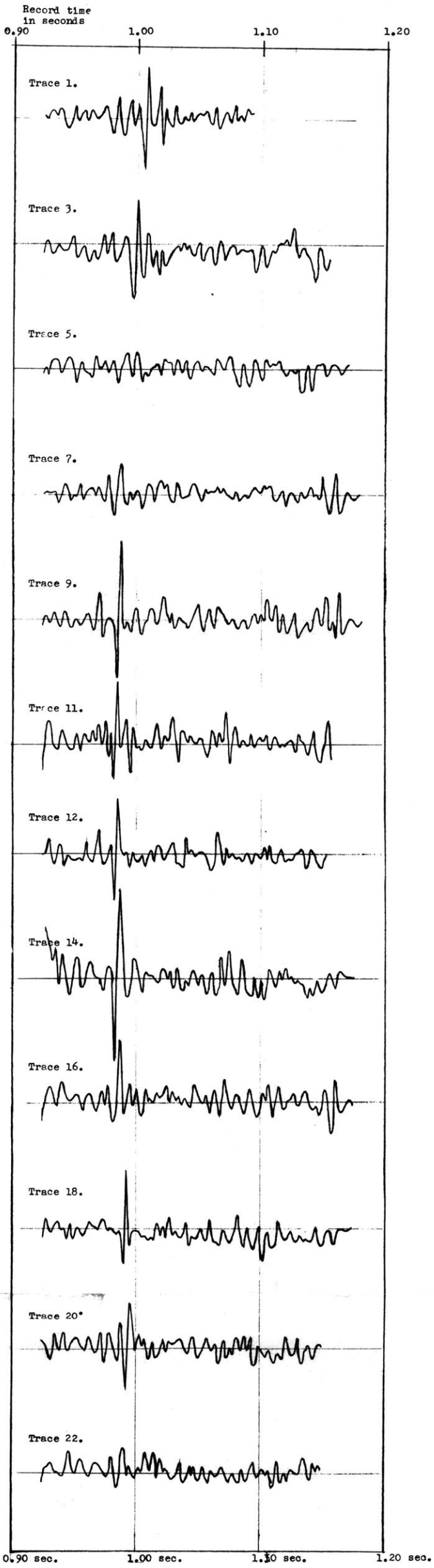

Fig. 3.24 A portion of record 7.19 filtered by symmetric operator formed from the sharp-front wavelet.

seconds, is not discernible. This is undoubtedly due to the extraneous amplitude content of the symmetric operator, which tends to emphasize any record noise present between events A and B, to the detriment of event B, whose amplitude is less than that of event A.

III.6. Conclusions and Recommendations

Although the inverse operator, either truncated, or modified in some form, has proven successful as a contractor, and, in the noise-free case, as a resolver, its usefulness on an actual seismogram appears to be limited by its sensitivity to noise and the shortness of its useable length.

Symmetric operators are able to give contraction, even in the presence of noise, but cannot be considered suitable resolvers. However, their application as resolvers on a piece-meal basis, in which separate symmetric operators would be used for each event of a complex is not unfeasible.

On the basis of experimental evidence, (the differences in the inverse wavelets, and spectral characteristics), the Ricker wavelet representation of a seismic reflection appears to be a rather poor approximation to physical reality. Admittedly this evidence is obtained from but one area, but examination of wavelets in other areas supports this conclusion.

Finally, it should be pointed out that the emphasis in this section has been on the development of methods whereby noise, in the form of the initial wavelet of the complex,

is filtered by contraction in order that the arrival times of later wavelets may be distinguished. Although these methods have not been satisfactorily effective in the area represented by the seismograms examined here, they may well prove to be the answer to the problem of resolution in other areas, where the wave forms of a complex are less diverse in character, and where the record noise level is not quite as high.

IV. THE REMOVAL OF NOISE IN THE INTERPRETATION OF POTENTIAL FIELD DATA - AN EXAMPLE OF A TWO-DIMENSIONAL OPERATOR

IV.1. Introduction

Prior to the translation of the potential field data into terms of the subsurface configuration, the usual objective of the interpreter is the preparation of a map of the residual field. This map is a representation of the potential field in which the potential due to the undesirable effects has been removed.

From our viewpoint, if we regard the observed data, $m(\underline{x})$, as a function of the two-dimensional variable $\underline{x} = (x_1, x_2)$, where x_1, and x_2 are the coordinates of the data point on a plane representing the earth's surface, and if we can in addition consider the data $m(\underline{x})$ as a linear combination of signal and noise, then preparation of a residual map is analagous to application of a two-dimensional filtering process, in which the observed data is filtered in such a way, as to remove the noise and leave the desired signal (residual anomaly). Hence, the problem of preparing the observed data for interpretation becomes the problem of designing a suitable two-dimensional filter for noise removal.

This chapter shall be concerned with the design of such filters, and their application to the interpretation of a gravity survey.

IV.2. Theory

The output of a two-dimensional filter, g_{ij}, at a point (i, j), for the discrete case, is given by

$$g_{i,j} = \sum_{s_1=-A}^{B} \sum_{s_2=-C}^{D} a_{s_1 s_2} m_{i-s_1, j-s_2} \qquad (2.2.1)$$

where the totality of terms $a_{s_1 s_2}$ is the two-dimensional filter or operator, and m_{ij} is the data input at the point (i, j). This can conveniently be expressed in matrix form, for

$$\begin{aligned} g_{ij} = {} & a_{-A,-C} m_{i+A,j+C} + \cdots + a_{0,-C} m_{i,j+C} + \cdots + a_{B,-C} m_{i-B,j+C} \\ & + a_{-A,-C+1} m_{i+A,j+C-1} + \cdots + a_{0,-C+1} m_{i,j+C-1} + \cdots \\ & \qquad + a_{B,-C+1} m_{i-B,j+C-1} \\ & + \cdots \\ & + \cdots \\ & + a_{-A,D} m_{i+A,j-D} + \cdots + a_{0,D} m_{i,j-D} + \cdots + a_{BD} m_{i-B,j-D} \end{aligned}$$

$$= \left[m_{i-k,j+C}\right]\left\{a_{k,-C}\right\} + \left[m_{i-k,j+C-1}\right]\left\{a_{k,-C+1}\right\} + \cdots$$

$$\cdots + \left[m_{i-k,j-D}\right]\left\{a_{k,D}\right\} \qquad (4.2.1)$$

$$k = -A, -A+1, \ldots, -1, 0, 1 \ldots, B-1, B$$

or, g_{ij} is the sum of (C + D + 1) matrix products of the form $\left[m_{i-k,j-\delta}\right]\left\{a_{k,\delta}\right\}$ where $\left[m_{i-k,j-\delta}\right]$ is a row matrix containing (A + B + 1) terms and $\left\{a_{k,\delta}\right\}$ is a column matrix with a similar number of terms, some of which may be zero.

Thus, g_{ij} may be considered the result of operating on our signal with (C + D + 1) one-dimensional operators. This is a convenient form for computation, especially for digital electronic computers.

g_{ij} as represented in (4.2.1), may be considered the product of two matrices, rather than a sum.

$$g_{ij} = \underline{m}\,\underline{a} \tag{4.2.2}$$

where

$$\underline{m} = \Big[m_{i+A,j+C},\ m_{i+A-1,j+C},\ \cdots,\ m_{i,j+C},\ \cdots\ m_{i-B,j+C};\ \ldots$$

$$\ldots;\ m_{i+A,j},\ \cdots,\ m_{ij},\ \cdots,\ m_{i-B,j};\ \ldots$$

$$\ldots;\ m_{i+A,j-D},\ \cdots,\ m_{i,j-D},\ \cdots,\ m_{i-B,j-D}\Big] \tag{4.2.3}$$

a row matrix of (C + D + 1)(A + B + 1) terms, and

$$\underline{a} = \Big\{a_{-A,-C},\ a_{-A+1,-C},\ \cdots,\ a_{0,-C},\ \cdots,\ a_{B,-C};\ \ldots;\ a_{-A,0},\ \cdots;$$

$$a_{00},\ \cdots,\ a_{B,0};\ \ldots;\ a_{-A,D},\ \cdots,\ a_{0,D}\ \ldots;\ a_{B,D}\Big\} \tag{4.2.4}$$

a column matrix of a similar number of terms.

Let us consider a region 2N x 2N, in which our data m_{ij} is defined, and let our operator a_{ij} be such that its extension in this region is 2M x 2M, with $M < N$ (or of extension 2N x 2N, with a sufficient number of terms on the

periphery of the region equal to zero). Then g_{ij} will be defined for $-(N-M) \leq i, j \leq (N-M)$.

If we consider the output along the row $i = r$, where

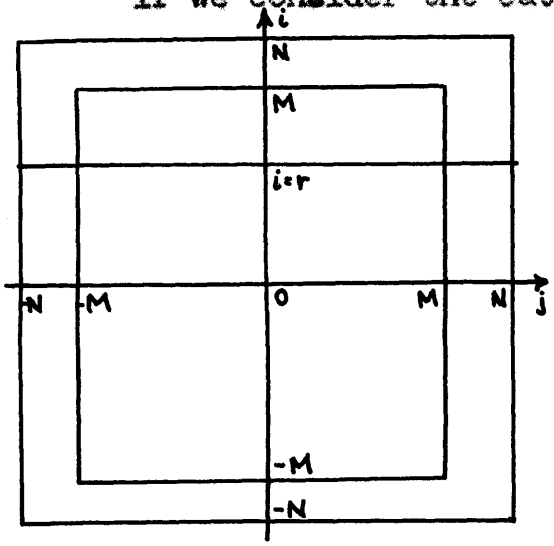

$-(N-M) \leq r \leq (N-M)$, and let the column matrix

$$\underline{g}_r = \left\{ g_{r,-(N-M)}, \; g_{r,-(N-M)+1}, \; \ldots, \; g_{r,0}, \; \ldots, \; g_{r,(N-M)} \right\} \quad (4.2.4)$$

represent the output along this row, then

$$\underline{g}_r = \underline{m}_r \underline{a} \quad (4.2.5)$$

where $\underline{m}_r$ is the rectangular matrix of data points.

$$\underline{m}_r = \begin{bmatrix} m_{r+M,N-2M} \cdots ; \cdots ; m_{r-M,N-2M} \cdots m_{r-M,N-M} \cdots m_{r-M,N} \\ \cdots\cdots\cdots\cdots\cdots\cdots\cdots\cdots\cdots\cdots\cdots\cdots\cdots\cdots\cdots\cdots\cdots\cdots \\ \cdots\cdots\cdots\cdots\cdots\cdots\cdots\cdots\cdots\cdots\cdots\cdots\cdots\cdots\cdots\cdots\cdots\cdots \\ m_{r+M,-M} \cdots ; \cdots ; m_{r-M,-M} \cdots m_{r-M,0} \cdots m_{r-M,M} \\ \cdots\cdots\cdots\cdots\cdots\cdots\cdots\cdots\cdots\cdots\cdots\cdots\cdots\cdots\cdots\cdots\cdots\cdots \\ \cdots\cdots\cdots\cdots\cdots\cdots\cdots\cdots\cdots\cdots\cdots\cdots\cdots\cdots\cdots\cdots\cdots\cdots \\ m_{r+M,-N} \cdots ; \cdots ; m_{r-M,-N} \cdots m_{r-M,-N+M} \cdots m_{r-M,-N+2M} \end{bmatrix} \quad (4.2.6)$$

in which each row of the matrix is of the form (4.2.3) representing the output due to one point on the row and the matrix $\underline{a}$ is of the form (4.2.5).

The output of the filter over the entire region is given by

$$\sum_{r} \underline{\varepsilon}_r = \sum_{r=-(N-M)}^{N-M} \underline{m}_r \underline{a}_r \qquad (4.2.7)$$

As was pointed out in Chapter III, the location of the signal (in this instance, the residual anomaly) is the primary consideration; its shape, although important, is not of immediate concern. This is particularly true in the interpretation of potential field data, where depth estimations, usually based on the inflection points of the residual anomaly, can only give a lower bound on the depth of the anomalous configuration. This is a consequence of the inherent ambiguity of the potential distribution, for the anomalous body may be replaced by a surface distribution of poles on an infinite plane between the body and the point of observation and still give rise to the same potential distribution at the observation point. As a consequence, retention of the anomaly shape after filtering is not significant.

If we choose to design our operator such that the location of our anomaly is to be indicated by a two-dimensional spike after filtering, then we have a similar situation to that of Chapter III.

Let us define our two-dimensional spike as unity at the centre of the anomaly, and zero everywhere else.

Then, if we consider an operator of extension 2M x 2M, the output of such a spiking operator $\underline{I}_r$ along the r^{th} row will be the column matrix

$$\underline{I}_r = \{0,\ 0,\ 0,\ \ldots\ldots,\ 0;\ 0,\ 0\} \qquad (4.2.8)$$

except for that row r = v in which the centre of anomaly lies. The output along this row will be the column matrix.

$$\underline{I}_{r=v} = \{0,\ 0,\ 0,\ \ldots,\ 0,\ 0,\ 1,\ 0,\ 0,\ \ldots,\ 0,\ 0,\ 0\}. \quad (4.2.9)$$

Then the output of the operator over the entire region 2N x 2N is given by

$$\sum_r \underline{I}_r = \sum_{r=-(N-M)}^{N-M} \underline{m}_r \underline{a} = \begin{bmatrix} 0, 0, \ldots, 0, 0, 0, \ldots, 0, 0 \\ \cdots\cdots\cdots\cdots\cdots\cdots\cdots \\ \cdots\cdots\cdots\cdots\cdots\cdots\cdots \\ 0, 0, \ldots, 0, 1, 0, \ldots, 0, 0 \\ \cdots\cdots\cdots\cdots\cdots\cdots\cdots \\ \cdots\cdots\cdots\cdots\cdots\cdots\cdots \\ 0, 0, \ldots, 0, 0, 0, \ldots, 0, 0 \end{bmatrix}. \quad (4.2.10)$$

Suppose our data $m_{ij} = s_{ij} + n_{ij}$, where s_{ij} is the signal corresponding to the anomaly and n_{ij}, the noise, and let us choose our operator such that the difference between our two-dimensional spike (4.2.10) and the output of the operation due to the input signal only, $\sum_r \underline{g}_r = \sum_r \underline{s}_r \underline{a}$ is to be minimized in a least squares sense.

Then we wish to minimize E^2, where

$$E^2 = \sum_{r=-(N-M)}^{N-M} (\underline{I}_r - \underline{g}_r)^2 \quad (4.2.11)$$

$$= \sum_r [\underline{I}_r - \underline{g}_r]^T [\underline{I}_r - \underline{g}_r] \quad (4.2.12)$$

where the superscript T, indicates the matrix transpose.

$$E^2 = \sum_r \left[\underline{I}_r^T\underline{I}_r - \underline{g}_r^T\underline{I}_r - \underline{I}_r^T\underline{g}_r + \underline{g}_r^T\underline{g}_r\right]. \qquad (4.2.13)$$

But $\underline{I}_r^T\underline{g}_r = (\underline{g}_r^T\underline{I}_r)^T$ is a scalar, since $\underline{I}_r$ and $\underline{g}_r$ are both column matrices, and the transpose of a scalar is the scalar itself. Therefore, $\underline{I}_r^T\underline{g}_r = \underline{g}_r^T\underline{I}_r$, and (4.2.13) becomes

$$E^2 = \sum_r \left[\underline{I}_r^T\underline{I}_r - 2\underline{g}_r^T\underline{I}_r + \underline{g}_r^T\underline{g}_r\right]. \qquad (4.2.14)$$

But, $\underline{g}_r = \underline{s}_r\underline{a}$ and $\underline{g}_r^T = \underline{a}^T\underline{s}_r^T$ and (4.2.14) becomes

$$E^2 = \sum_r \left[\underline{I}_r^T\underline{I}_r - 2\underline{a}^T\underline{s}_r^T\underline{I}_r + \underline{a}^T\underline{s}_r^T\underline{s}_r\underline{a}\right]. \qquad (4.2.15)$$

Now, for a minimum $\delta E^2 = 0$

$$\delta E^2 = \sum_r \left[-2\delta(\underline{a}^T)\underline{s}_r^T\underline{I}_r + \delta(\underline{a}^T)\underline{s}_r^T\underline{s}_r\underline{a} + \underline{a}^T\underline{s}_r^T\underline{s}_r\delta(\underline{a})\right]. \qquad (4.2.16)$$

But, as before, $\underline{a}^T\underline{s}_r^T\underline{s}_r\delta(\underline{a}) = \left[\delta(\underline{a}^T)\underline{s}_r^T\underline{s}_r\underline{a}\right]^T$ is a scalar, and hence (4.2.16) becomes

$$\delta E^2 = 2\sum_r \left[-\delta(\underline{a}^T)\underline{s}_r^T\underline{I}_r + \delta(\underline{a}^T)\underline{s}_r^T\underline{s}_r\underline{a}\right]. \qquad (4.2.17)$$

Hence, for a minimum,

$$\sum_r \delta(\underline{a}^T)\underline{s}_r^T\underline{s}_r\underline{a} = \sum_r \delta(\underline{a}^T)\underline{s}_r^T\underline{I}_r \qquad (4.2.18)$$

or

$$\left[\sum_r \underline{s}_r^T\underline{s}_r\right]\underline{a} = \sum_r \underline{s}_r^T\underline{I}_r, \qquad (4.2.19)$$

since $\underline{a}$ is independent of r, and where we assume the elements of $\delta(\underline{a})^T$ are independent.

Let us assume that the inverse of the matrix $\sum_r \underline{s}_r^T \underline{s}_r$ exists. Hence, if we premultiply both sides of (4.2.19) by $\left[\sum_r \underline{s}_r^T \underline{s}_r\right]^{-1}$, then we have

$$\underline{a} = \left[\sum_r \underline{s}_r^T \underline{s}_r\right]^{-1} \sum_r \underline{s}_r^T \underline{I}_r \quad . \qquad (4.2.20)$$

Other criteria, such as the minimization of the ratio of the output power of the noise (n_{ij}) to the output power of the data (m_{ij}), require prior knowledge of the noise distribution over the data space, and as such, determination of the suitable operator is superfluous, for if the noise distribution is known, then the desired signal may be determined by subtraction directly.

In this instance, (4.2.20) specifies the desired operator in terms of signal shape only, regardless of the location of the signal in the data space.

IV.3. The Derivation of the Spiking Operator for the Anomaly Due to a Buried Sphere, and Its Application to the Detection of such an Anomaly in the Presence of Noise

The anomaly or signal chosen was the gravitational field due to a spherical mass of density contrast unity. The depth to the centre of mass of the sphere is 1,000 metres, and its radius is 500 metres. Figure 4.1 illustrates the potential distribution due to such a mass.

To facilitate computation, a 1 x 1 operator was chosen; this operator will contain five terms

$$\underline{a} = \left\{a_{-1,0},\ a_{+1,0},\ a_{00},\ a_{0,+1},\ a_{0,-1}\right\}.$$

In view of the circular symmetry of the signal, the operator coefficients $a_{-1,0}$, $a_{+1,0}$, $a_{0,+1}$, and $a_{0,-1}$ will be equal, and, hence, determination of the operator, according to (4.2.20) requires but the inversion of a 2 x 2 matrix. (Fig. 4.3).

The two-dimensional autocorrelation function of the signal, for eight lags for one-quarter of the map area of Figure 4.1 is illustrated in Figure 4.4. It, too, exhibits central symmetry, as was to be expected. Slight variations in this symmetry are undoubtedly due to round-off errors.

The two-dimensional wave-number spectrum of the signal is illustrated in Figure 4.5. The power is concentrated in the region of low wave-numbers, or, high wave-lengths, and rapidly falls off to zero in the region of high wave-numbers.

Computation of the two-dimensional spectra was facilitated by taking advantage of the even function properties of the autocorrelation function, for

$$\Phi_{11}(k_1, k_2) = \sum_{s_1=-8}^{+8} \sum_{s_2=-8}^{+8} \varphi_{11}(s_1, s_2) e^{-i(k_1 s_1 + k_2 s_2)} \qquad (2.2.12)$$

$$= \varphi_{11}(0, 0) + 2\sum_{s_1=1}^{8} \varphi_{11}(s_1, 0)\cos k_1 s_1 + 2\sum_{s_2=1}^{8} \varphi_{11}(0, s_2)\cos k_2 s_2$$

$$+ 4\sum_{s_1=1}^{8} \sum_{s_2=1}^{8} \varphi_{11}(s_1, s_2)\cos k_1 s_1 \cos k_2 s_2. \qquad (4.3.1)$$

Figure 4.6 illustrates the autocorrelation function of our operator (Fig. 4.3). Again only one-quarter of the map area was used in the computation of the autocorrelation function because of the central symmetry of the operator.

The wave-number spectrum of the operator is illustrated in Figure 4.7. Equation (4.3.1), with suitable limits was again used to compute the spectrum. The power here is concentrated in the region of high wave-numbers, and falls off fairly rapidly to zero in the region of low wave-numbers. Thus, the spectrum of our spiking operator approximates the inverse of the spectrum of the signal--the design criterion that was used to determine the resolution operator in one dimension.

Figure 4.8 shows the result of convolving our operator with the signal of Figure 4.1. Definition of the centre of the anomaly is immediate. The anomaly or signal, originally 4 kms. wide, has been compressed by this operator to a width of but 2 kms. Section A-A' (Fig. 4.10) illustrates this compression.

The operator was then used to detect the existence of the anomaly of Figure 4.1 in the presence of noise in the form of a south regional gradient of 40 gravity units per kilometre. Figure 4.2 illustrates this combined field. (The data for Figures 4.1 and 4.2 was obtained from Agocs (1951)). The presence of the anomaly is indicated by

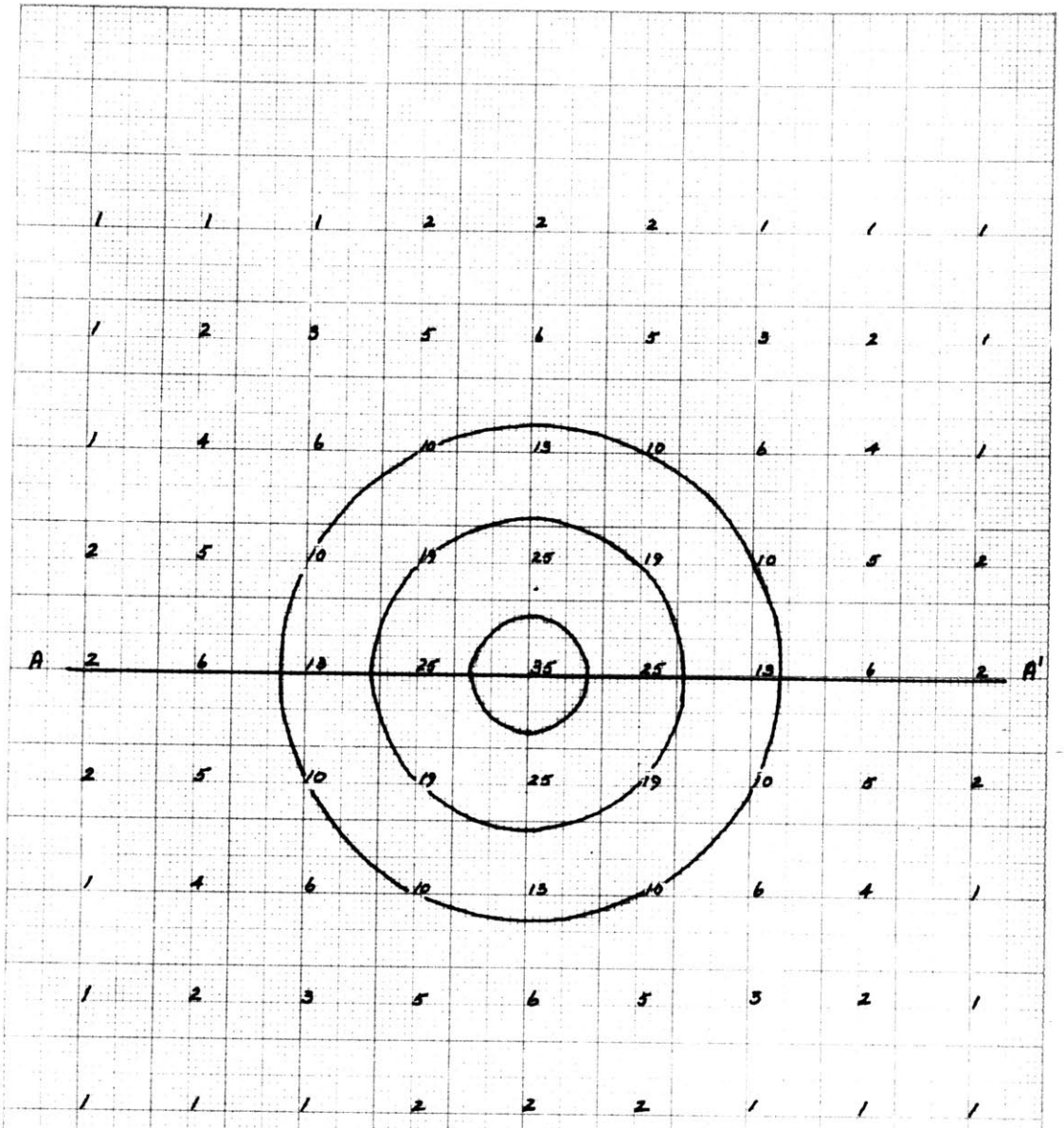

Contour interval: 10 units.
Scale: 1½" = 1Km.

Fig. 4·1. Anomaly or Signal due to Buried Sphere.

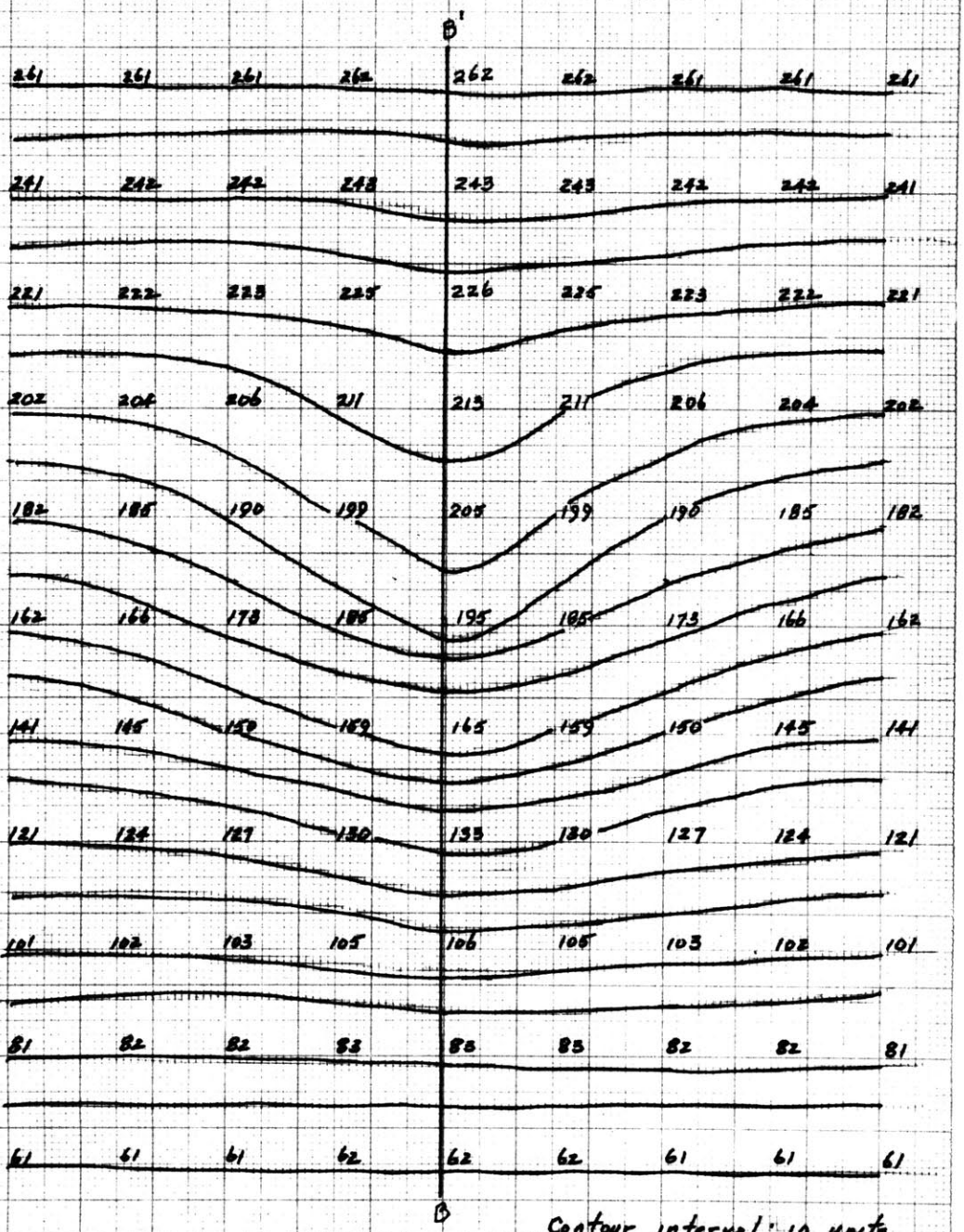

Fig 4.2. The Combined field of a Buried Sphere and a South Gradient of 40 gravity units per kilometre.

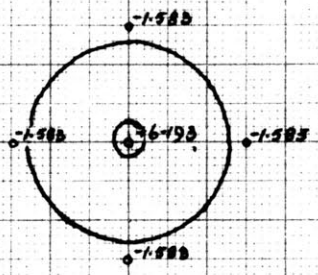

Contour interval: 5 units.
Scale: 1½" = 1km.

Fig. 4.3. The Operator, Derived by Applying the Least Squares Criterion.

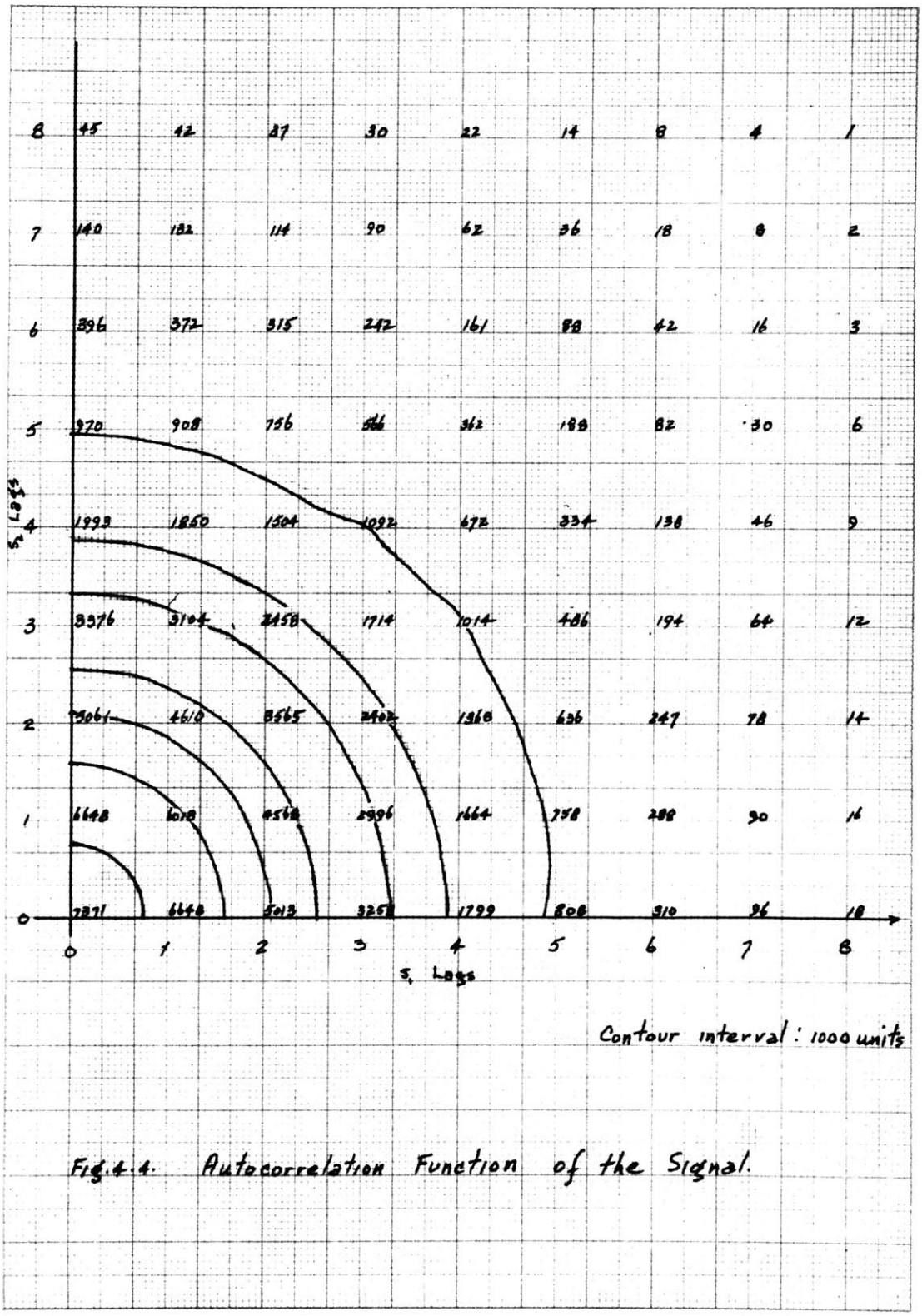

Fig. 4.4. Autocorrelation Function of the Signal.

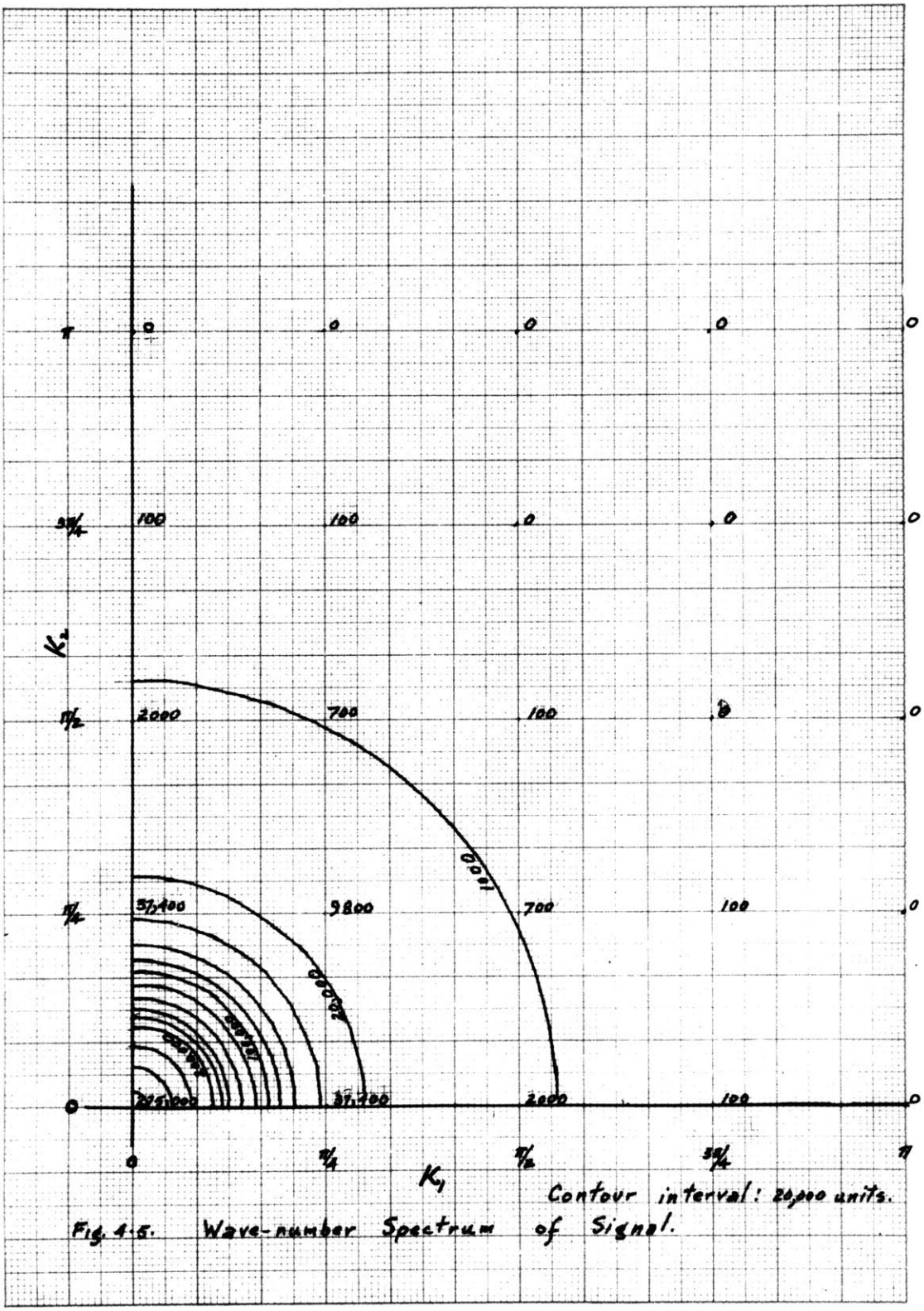

Fig. 4.5. Wave-number Spectrum of Signal.

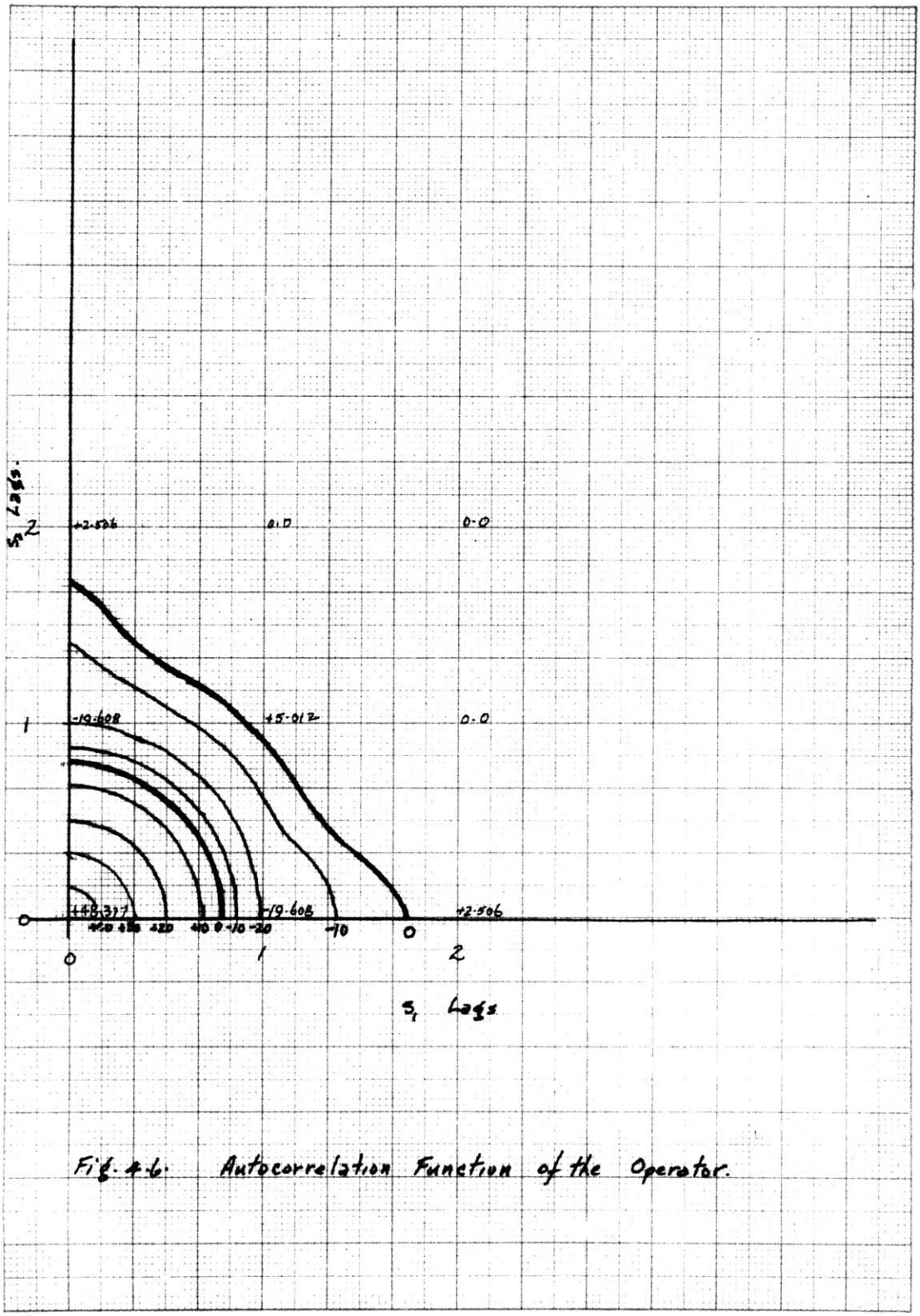

Fig. 4.6. Autocorrelation Function of the Operator.

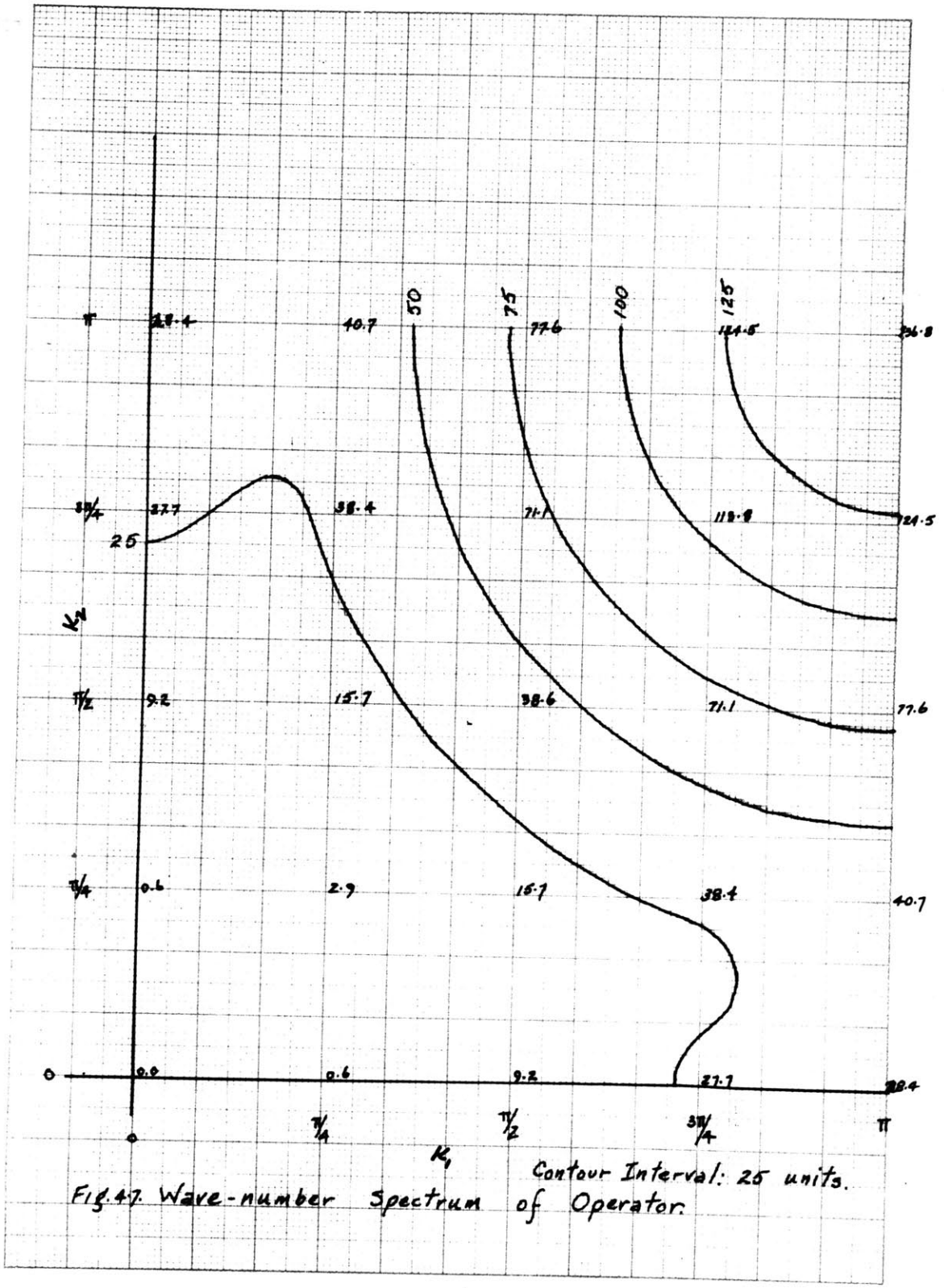

Contour Interval: 25 units.

Fig. 4.7. Wave-number Spectrum of Operator.

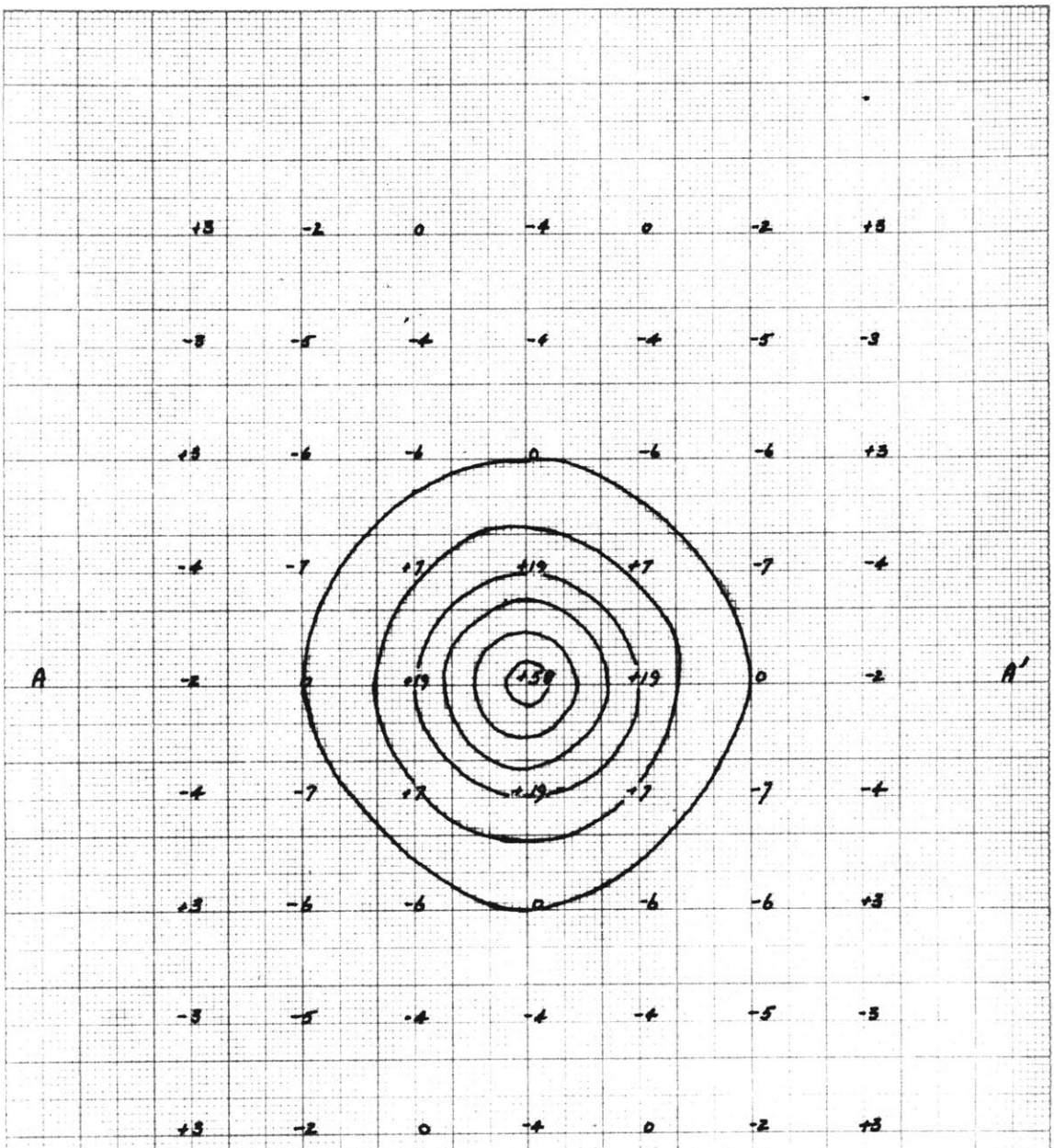

Fig. 4.8. Operator Convolved with Signal.

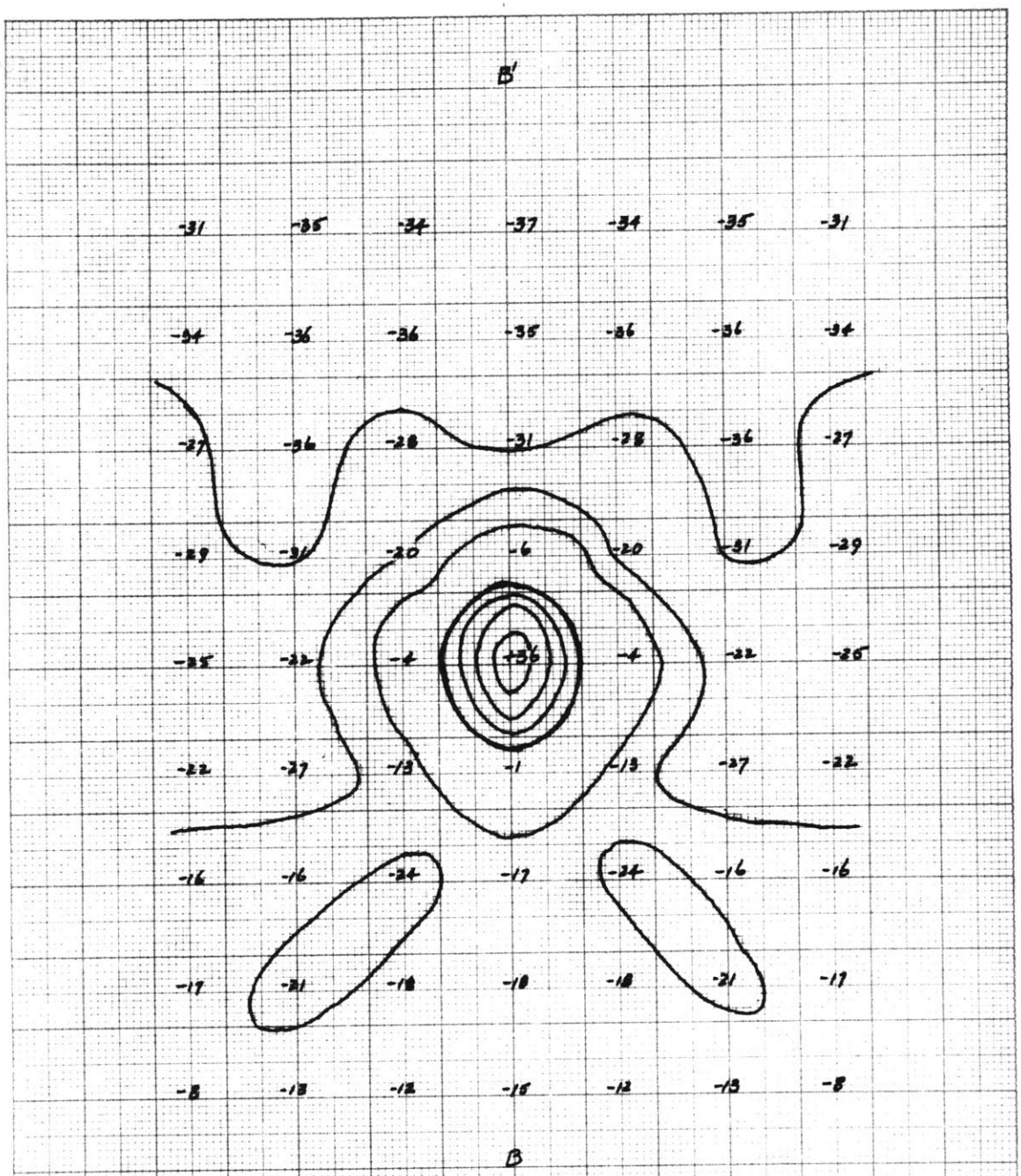

Contour interval: 10 units.
Scale: 1½" = 1 km.

Fig. 4.9. Operator Convolved with the Combined Field.

a slight nose. Its exact location would be difficult to determine. However, convolution of our operator with this combined field, as illustrated in Figure 4.9, clearly indicates the position of the anomaly. Section B-B', (Fig. 4.11) exhibits the compression, and the resulting sharper distinction between the anomaly and the superimposed regional field effect.

IV.4. Conclusions and Recommendations

Undoubtedly, in this simple case, the two-dimensional operator, derived according to the criterion of (IV.2) has proven to be a suitable detector of the signal in the presence of noise.

Its effectiveness in the presence of noise of a more complex nature, such as variation in the shape of the anomaly, or overlapping anomalies, remains to be investigated. However, we are inclined to think that the two-dimensional operator will be less sensitive to noise than the one-dimensional operator, primarily because of the smoothness of the observational data in potential field investigations.

It should be noted that the operator coefficients derived according to this criterion, for the anomaly examined, are approximately in the ratio of 4:1; that is, the central term a_{00} is approximately four times the symmetric terms. Now, the operator used to obtain the second derivative of the potential field also is such that the central term a_{00} is

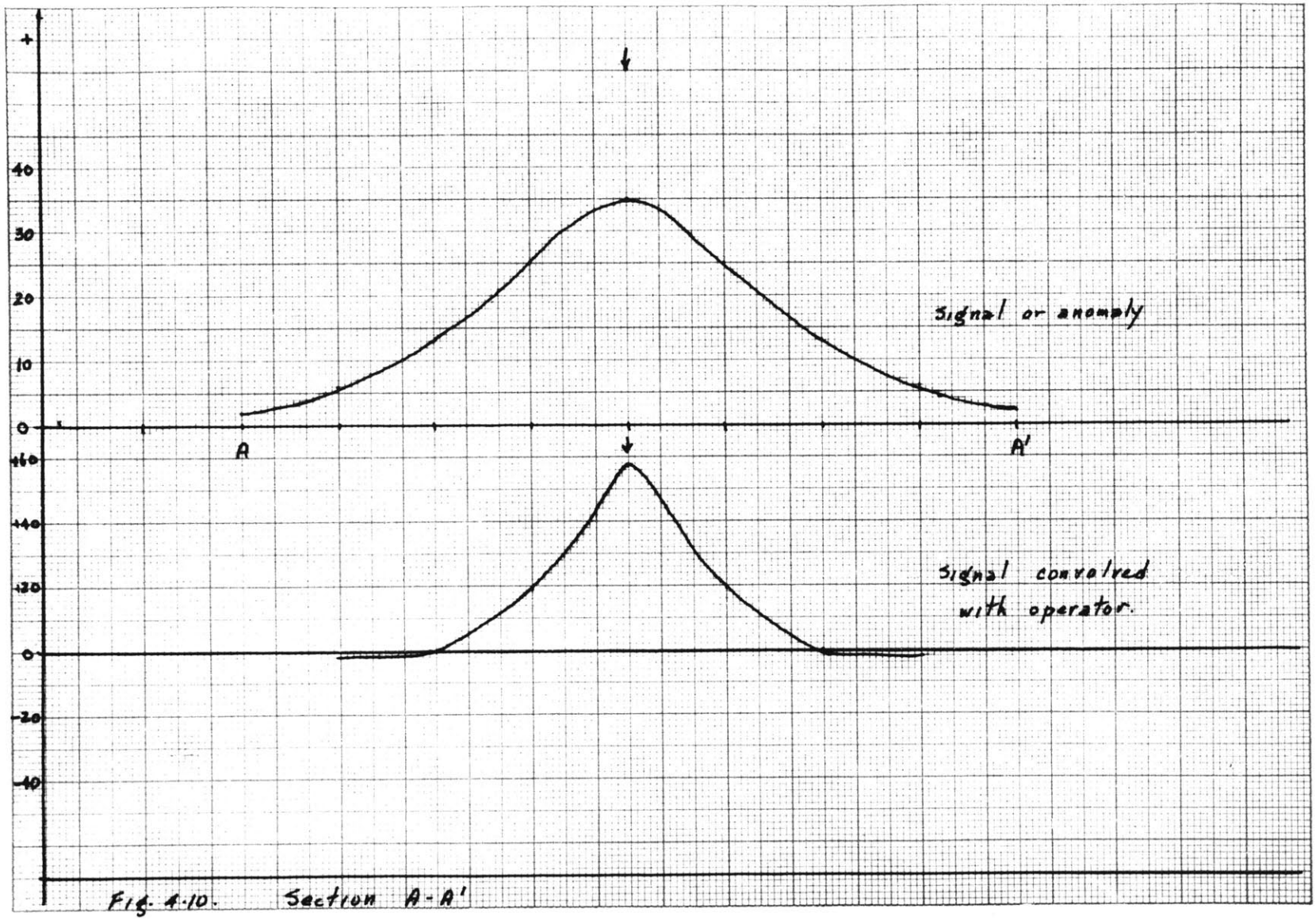

Fig. 4.10. Section A-A'

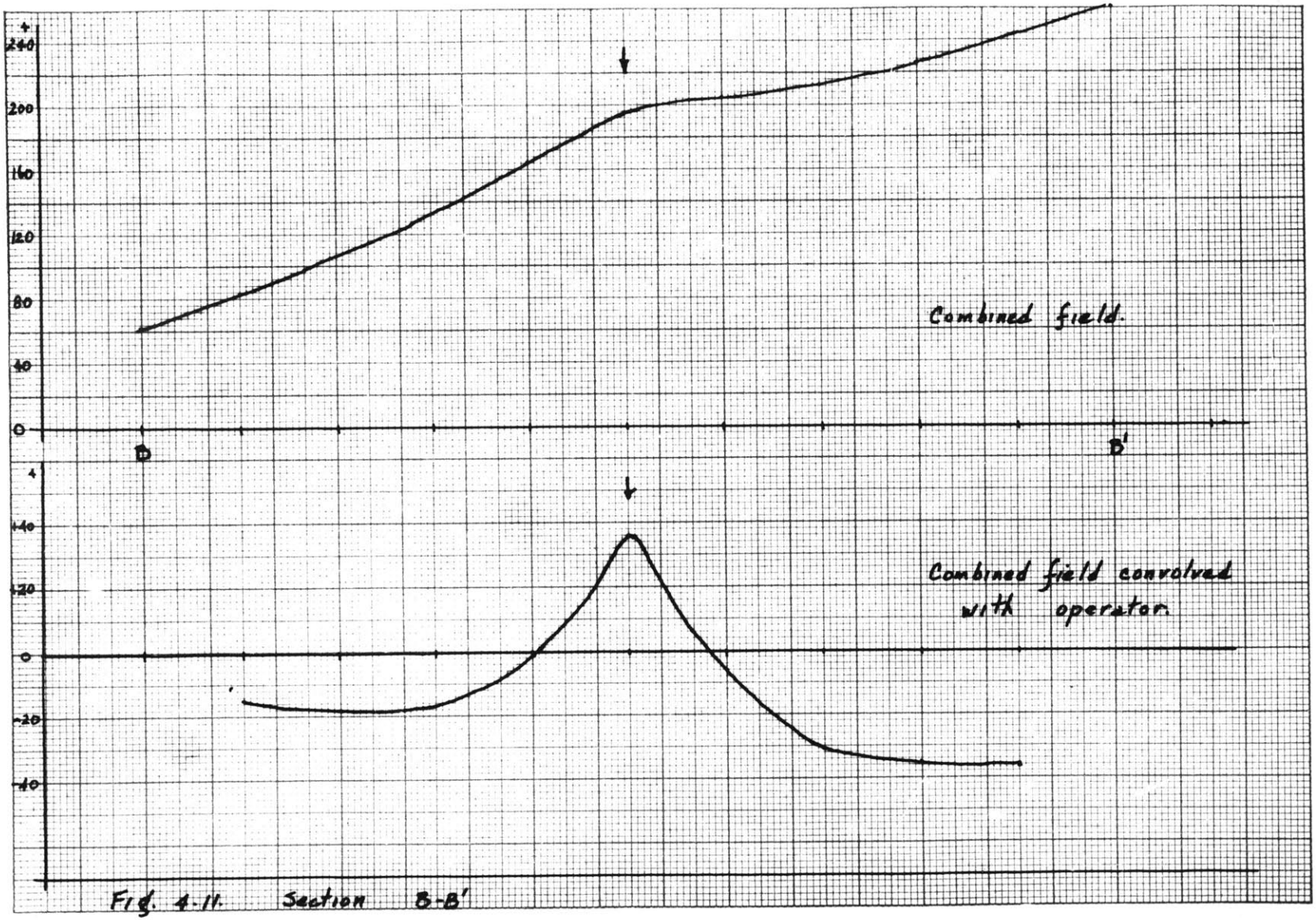

Fig. 4-11. Section B-B'

-four times the symmetric terms. Whether this is a mere coincidence due to the symmetrical form of the anomaly chosen, or whether there is some relationship between two-dimensional filtering of potential fields and their second derivatives, remains for further investigation.

From a practical viewpoint, the application of such operators in the interpretation of potential data would entail the formation of a library of operators corresponding to various types of anomalies. From the two-dimensional spectra of the observed data, some idea of the type of anomaly, if present, could be obtained, and then, after a choice from the library, of the corresponding operator, detection of the anomaly could be achieved by convolution.

Admittedly, the computation of spectra and non-symmetrical operators would be voluminous. For example, computation of a five-term operator requires inversion of a 5 x 5 matrix, which takes approximately three man-hours with a desk calculator. However, with high-speed electronic digital computers, the amount of calculation involved should offer no deterrent to the application of two-dimensional operators to potential field interpretation.

V. CONCLUDING REMARKS

The concept of considering observational data to consist of desirable signal plus obscuring noise is not necessarily restricted to geophysical data, but can certainly be extended to other scientific data.

The value of representing such data in the frequency domaine, or wave-number domaine, is necessarily dependent upon the use to which the data is to be put. However, in a predominantly observational science, such as geology, in which the emphasis is often on obtaining data trends, representation of the data in the wave-number domaine should prove to be a useful interpretative tool.

In the studies made in this thesis, the two-dimensional operator has proven to be more successful in its purpose than the one-dimensional operator. This conclusion must be considered in light of the data examined, for without doubt the seismogram is a much more complex representation of nature than the gravity field data examined.

It should also be pointed out that the aspects of the filter theory presented here are relevant only for data which can be considered a <u>linear</u> combination of signal and noise. Perhaps the limitation in the success of our one-dimensional operator for the seismogram lies in the digression from linearity of the signal and noise relation.

Effective operators for such data lie, no doubt, in the field of non-linear filters, in which some work is being done at present at the Massachusetts Institute of Technology.

REFERENCES

Agocs, W. B. 1951 Least Squares Residual Anomaly Determination, Geophysics, 16, pp. 686-696.

Geophysical Analysis Group, M.I.T., Report No. 9, 1955.

Guillemin, E. A. 1948 Mathematics of Circuit Analysis, (Technology Press, Cambridge, Massachusetts).

Lee, Y. W. 1955 Statistical Theory of Communication, unpublished lecture notes.

Piety, R. G. 1955 Personal communication.

Ricker, N. 1953a The Form and Laws of Propagation of Seismic Wavelets, Geophysics, 18, pp. 10-40.

_____ 1953b Wavelet Contraction, Wavelet Expansion, and the Control of Seismic Resolution, Geophysics, 18, pp. 769-792.

Robinson, E. A. 1954 Predictive Decomposition of Time Series with Applications to Seismic Exploration, M.I.T. GAG Report No. 7.

Schwartz, C. A. 1954 Some Geometrical Properties of Residual Maps, Geophysics, 19, pp. 46-70.

Smith, M. K. 1954 Filter Theory of Linear Operators with Seismic Applications, Ph.D. Thesis, M.I.T. (M.I.T. GAG Report No. 6).

Titchmarsh 1948 Introduction to the Theory of the Fourier Integral, (Clarendon Press, Oxford, Edition 2).

Wiener, N. 1950 Extrapolation, Interpretation and Smoothing of Stationary Time Series, (Technology Press, Cambridge, Massachusetts).